

## **Supplemental Data**

### **EEG Responses to Visual Landmarks in Flying Pigeons**

Alexei L. Vyssotski, Giacomo Dell’Omo, Gaia Dell’Ariccia, Andrei N. Abramchuk, Andrei N. Serkov, Alexander V. Latanov, Alberto Loizzo, David P. Wolfer, and Hans-Peter Lipp

Supplemental Figures

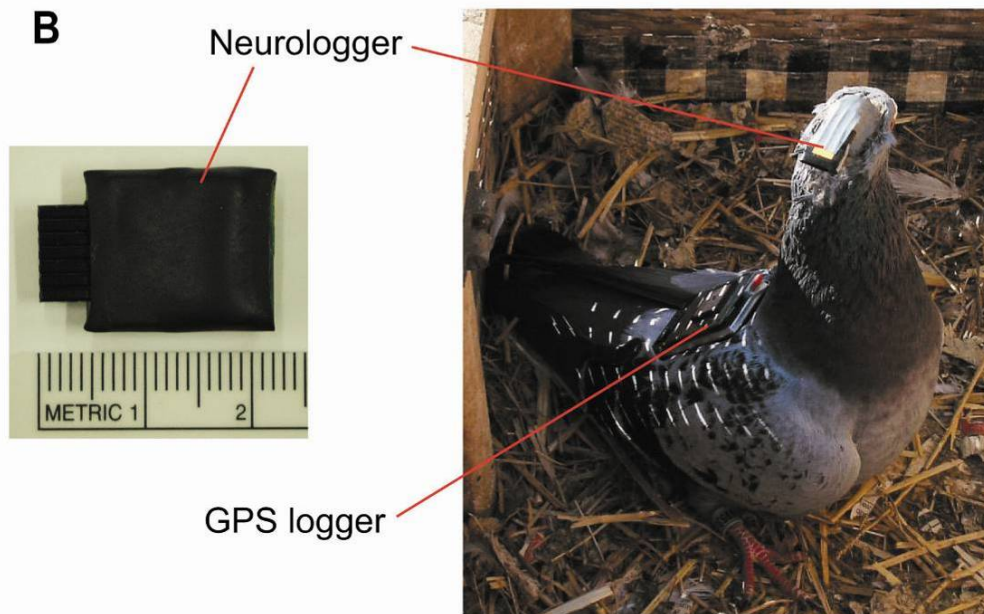
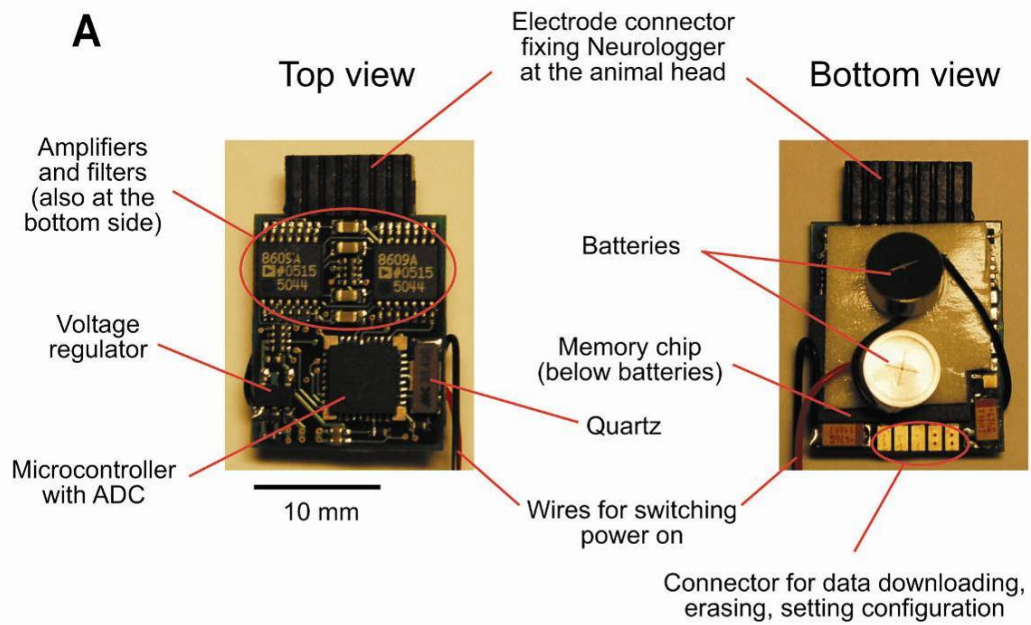


Figure S1. **Neurologger.** (A) Photograph of the Neurologger circuit boards. (B) Photograph of the Neurologger (in rubber protection) ready to be attached to the animal and attachment of the Neurologger and the GPS logger on the pigeon.

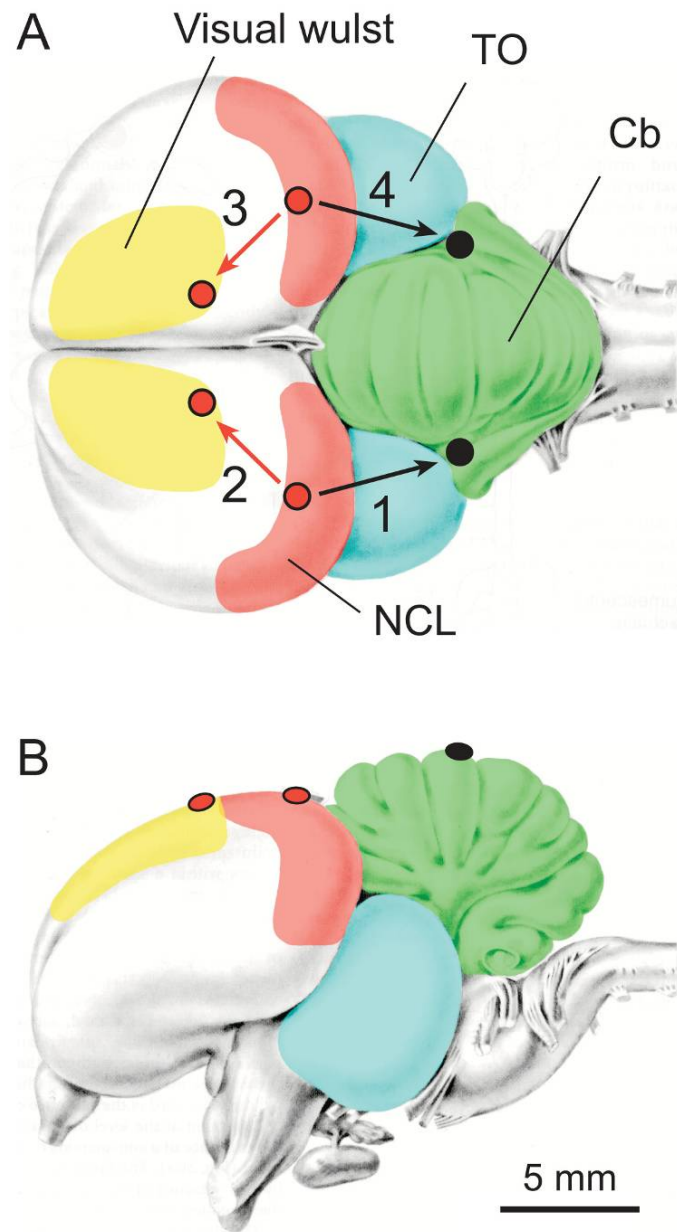
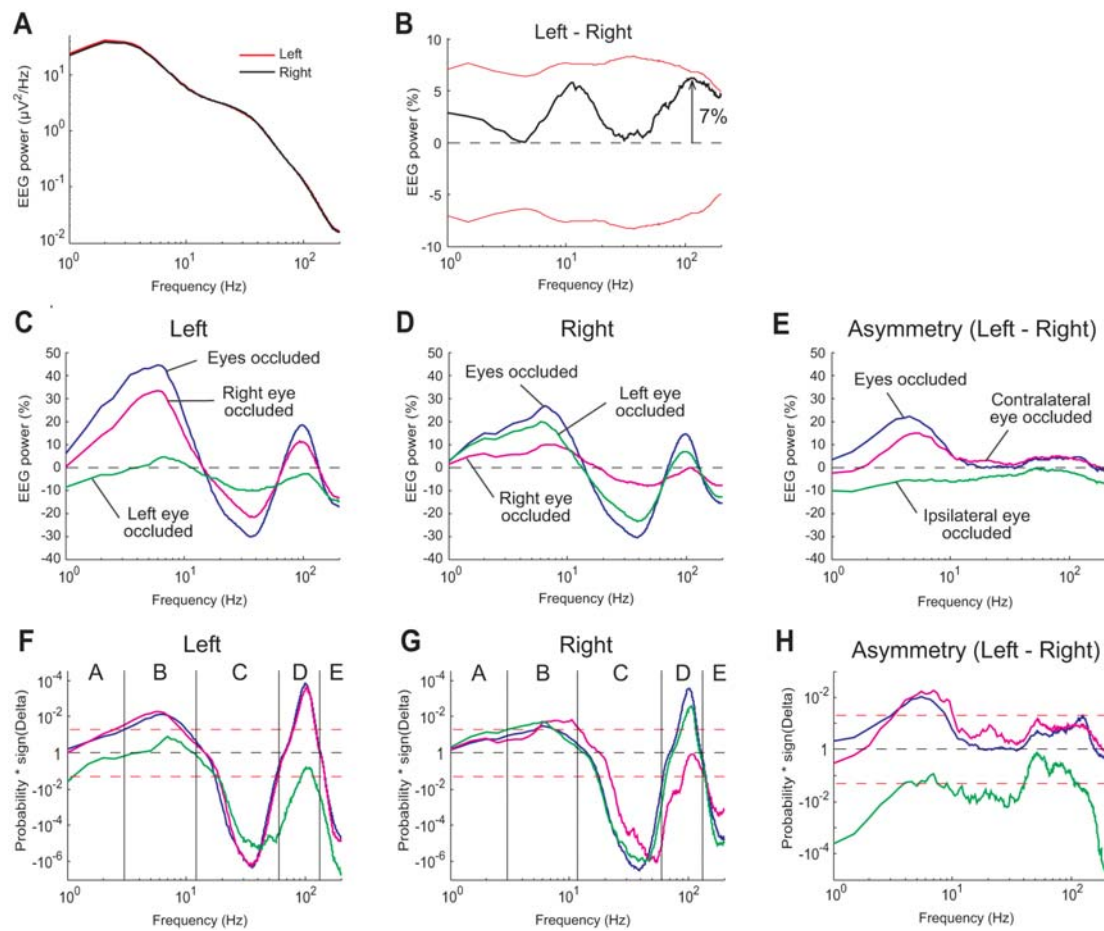
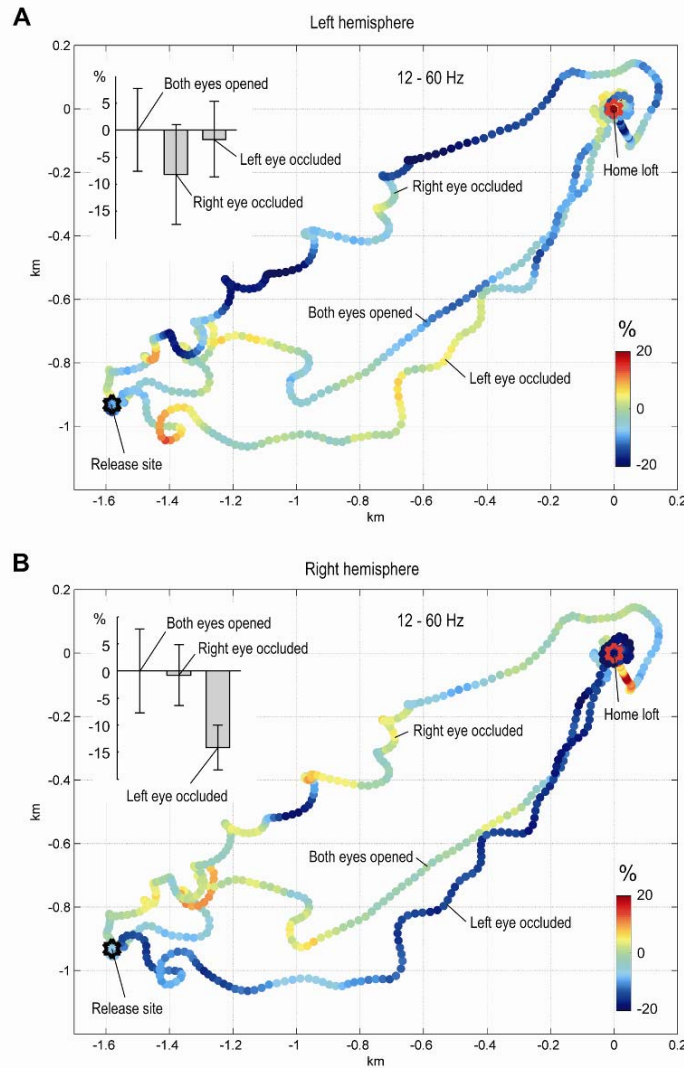


Figure S2. **Electrode placements as related to structures of the pigeon brain.** (A) Coronal view. (B) Lateral view. Colored circles indicate location of epidural electrodes for EEG recording in the current study. Differential signals between electrodes connected by the red arrows (labelled 2 and 3) were analyzed. Abbreviations: TO – *Tectum opticum*, Cb – *Cerebellum*, NCL – *Nidopallium caudolaterale*. The visual wulst is said to be equivalent of the striate cortex in mammals [26]. NCL has similar functions with the mammalian cortical-like regions, suggestively with the dorsal lateral prefrontal cortex [27]. Electrodes were placed in a way to pick up signals from both of these regions.



**Figure S3. Unilateral visual stimulation cause marked asymmetry in the pigeon's EEG, whereas the internal functional brain asymmetry has only moderate impact.** (A) EEG power spectrum from the left and the right hemispheres with both eyes open. This normal state is taken as reference. (B) Difference between left and right EEG power expressed in percents from the mean of two hemispheres. Red lines shows the standard deviation. (C – D) Influence of eye occlusion on EEG power in the right and left hemispheres (in %). (E) Asymmetry – difference between charts C – D. (F – G) Probability of deviation from the reference state multiplied by the sign of deviation, for the left and the right hemispheres respectively (two-tailed *t*-test). (H) The same as (F – G) but for the deviation of the left hemisphere from the right - probability for asymmetry (E). See Supplemental Results for additional description and comments.



**Figure S4. Eye occlusion decreases C range (12-60Hz) EEG power in the contralateral hemisphere of the flying pigeon.** (A) Color-coded EEG power in the left hemisphere along a pigeon's path. (B) Color-coded EEG power in the right hemisphere along a pigeon's path. The color along the flight trajectories represent deviation from the average of the flight with both eyes opened. The bird was released three times from the same location at one hour intervals: the first time with both eyes opened, the second time with the right eye occluded and the third time with the left eye occluded. Weighted power (i.e. different frequencies were pooled with different weight coefficients, see Supplemental Experimental Procedures for details) was calculated for one-second epochs, smoothed by a moving average with a span of 15 sec for better representation. Flight coordinates were recorded by the GPS logger every second. The bar charts of insets show the mean EEG power of the flight and standard deviation of one-second epochs in the flight. Like in the in-cage experiment (Figure S3), eye occlusion clearly reduced 12-60 Hz EEG power in the contralateral hemisphere of the flying pigeon, and practically did not affect activity of the ipsilateral hemisphere. As found in earlier studies with monocular occlusion [28], when the pigeon was flying with one eye occluded, it had a tendency to deviate from the shortest way to the home loft in the direction of the open eye, but corrected this deviation afterwards.

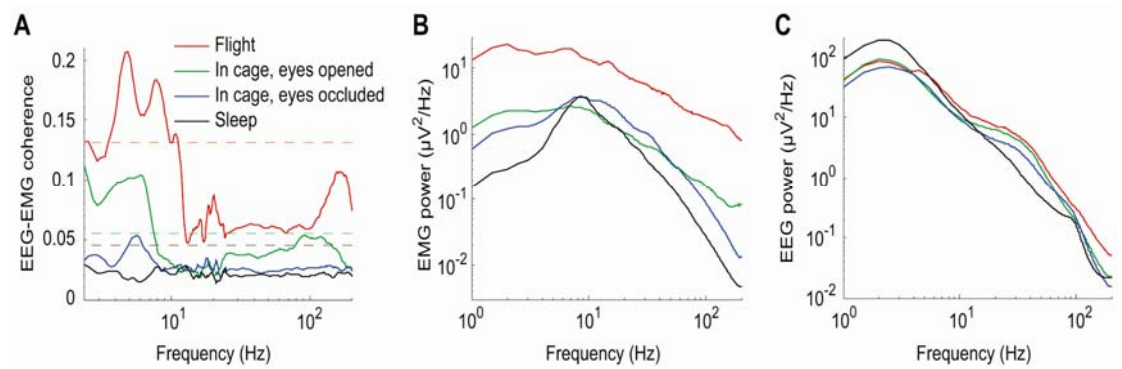


Figure S5. **EEG in A (0-3 Hz) and B (3-12 Hz) frequency ranges is coherent with the neck electromyogram.** (A) EEG-EMG coherence. Dotted lines mark  $P = 0.05$  for different states according to their colors (exception: blue  $\rightarrow$  green). (B) EMG power spectra. (C) EEG power spectra. See Supplemental Results for additional description and comments.

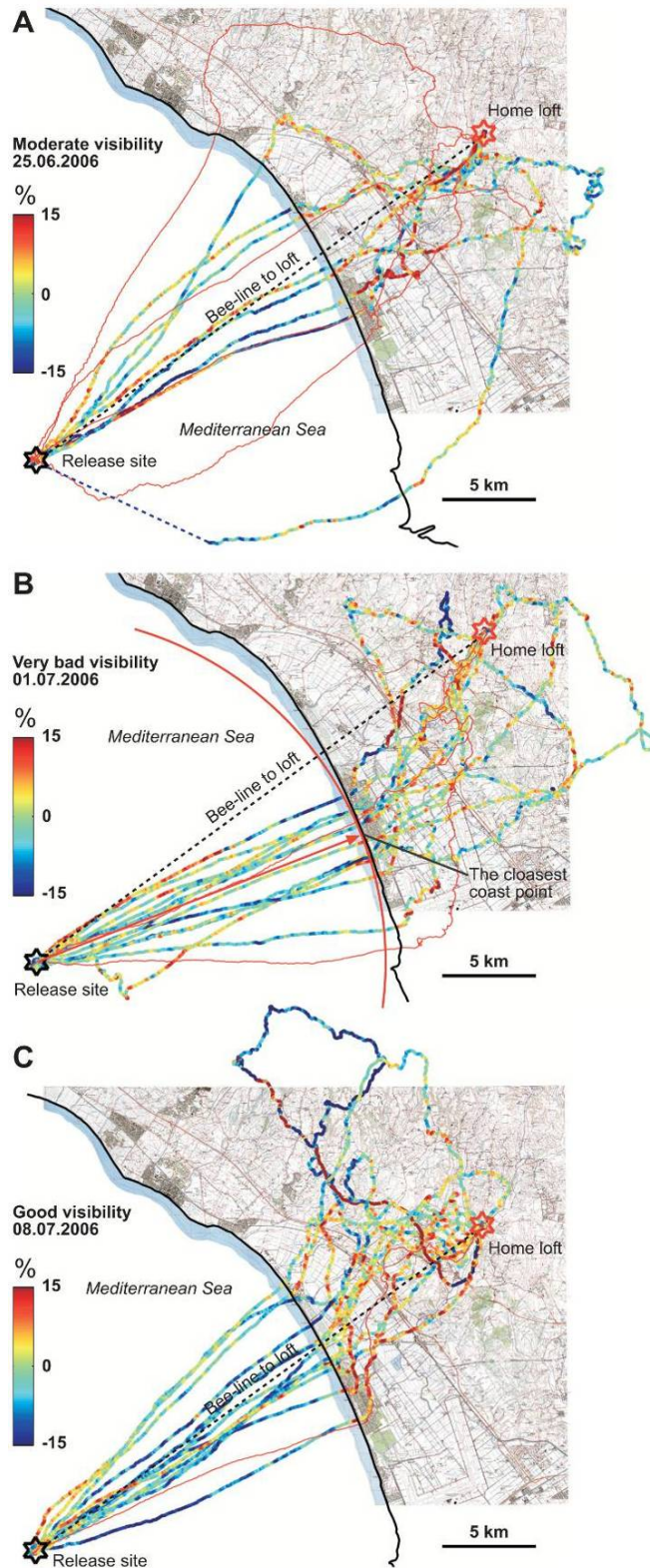
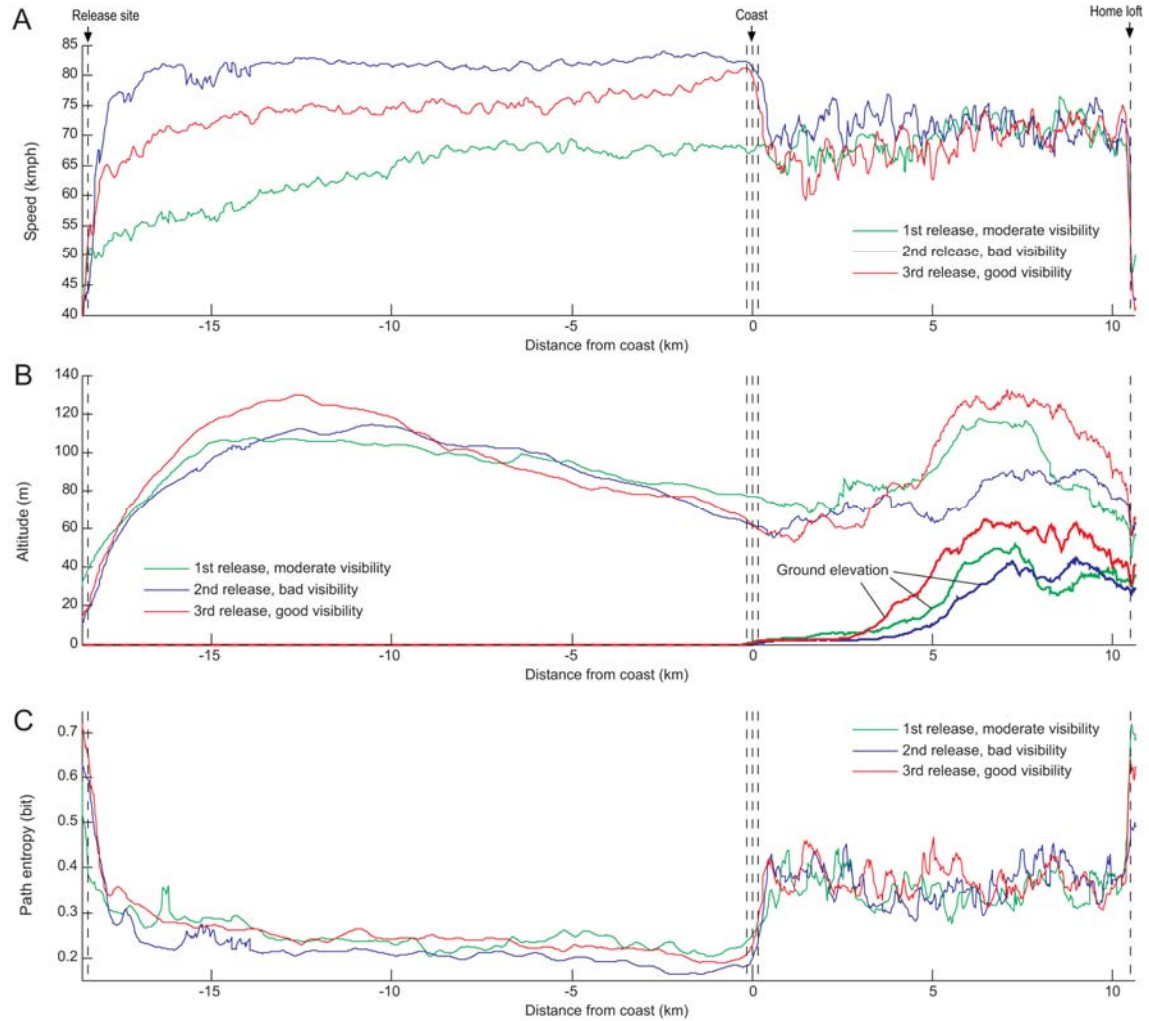


Figure S6. **Trajectories of pigeons in three sequential releases from the sea.** (A) First release in conditions of moderate visibility (8.2 km). (B) Second release in conditions of very bad visibility (6.0 km). (C) Third release in conditions of good visibility (10.3 km). Color codes EEG power in C (12-60 Hz) frequency range. Tracks without EEG records are shown by red lines.



**Figure S7. Flight parameters of pigeons in three sequential releases from the sea.** (A) Speed. (B) Altitude. (C) Path entropy. Horizontal scale indicates distance to the coast. Significant difference in flight speed over sea is notable. There were no differences in other parameters between releases. In (B) the ground elevation profiles were calculated as a mean of ground elevation on pigeon's paths on particular day. Color of the ground elevation chart corresponds to color of the flight altitude chart. On three different days pigeons took slightly different routes. For this reason three ground elevation profiles do not coincide.

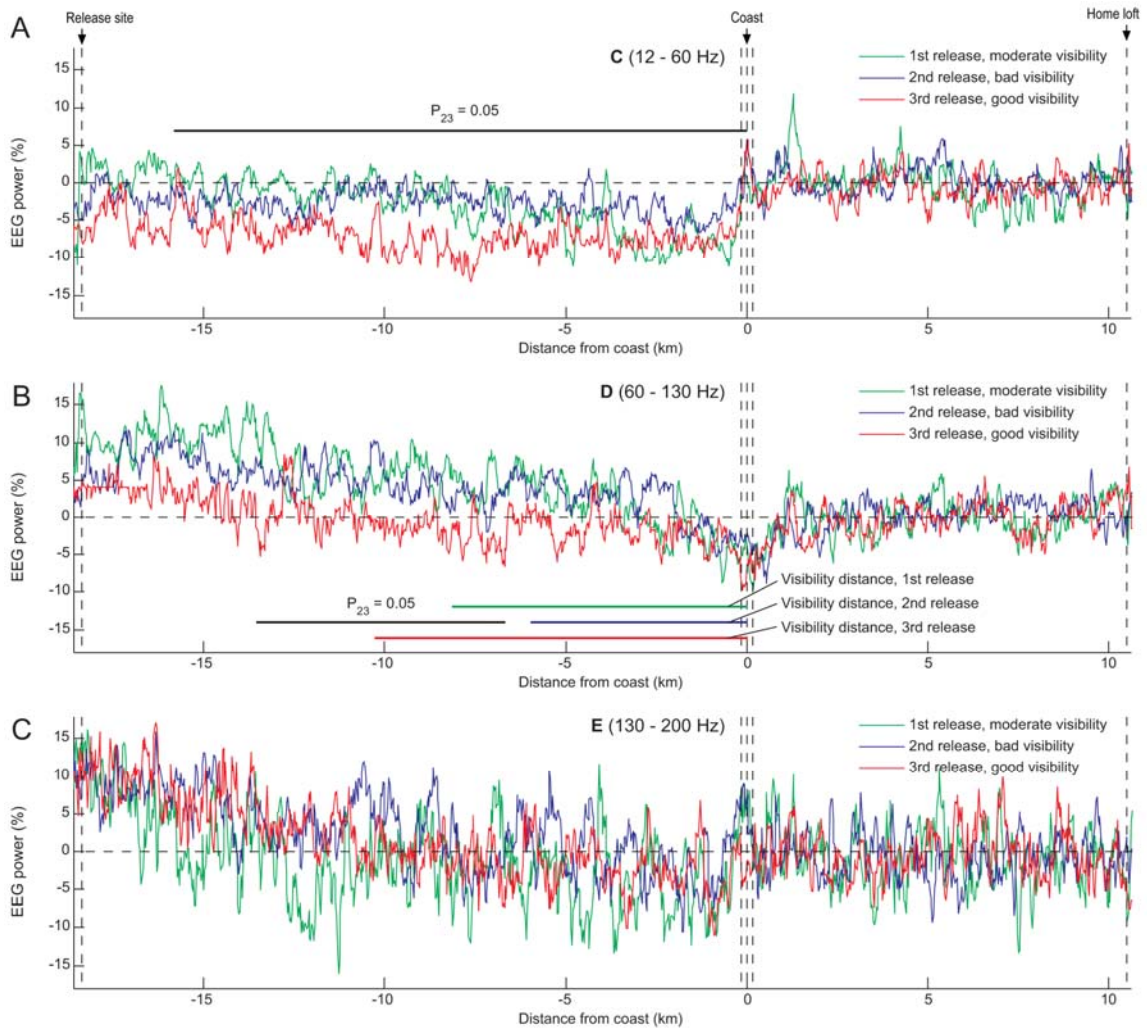


Figure S8. **EEG power in C, D and E frequency bands in releases over the sea.** (A) C band (12-60 Hz). (B) D band (60-130 Hz). (C) E band (130-200Hz). Intervals of significant difference between two releases in bad and good visibility conditions are marked by horizontal black bars in (A) and (B) (C and D bands). No significant difference in (C) was observed (E band). Visibility distances for humans evaluated by Fiumicino airport weather station are shown by green (moderate visibility), blue (bad visibility) and red (good visibility) horizontal bars in (B).

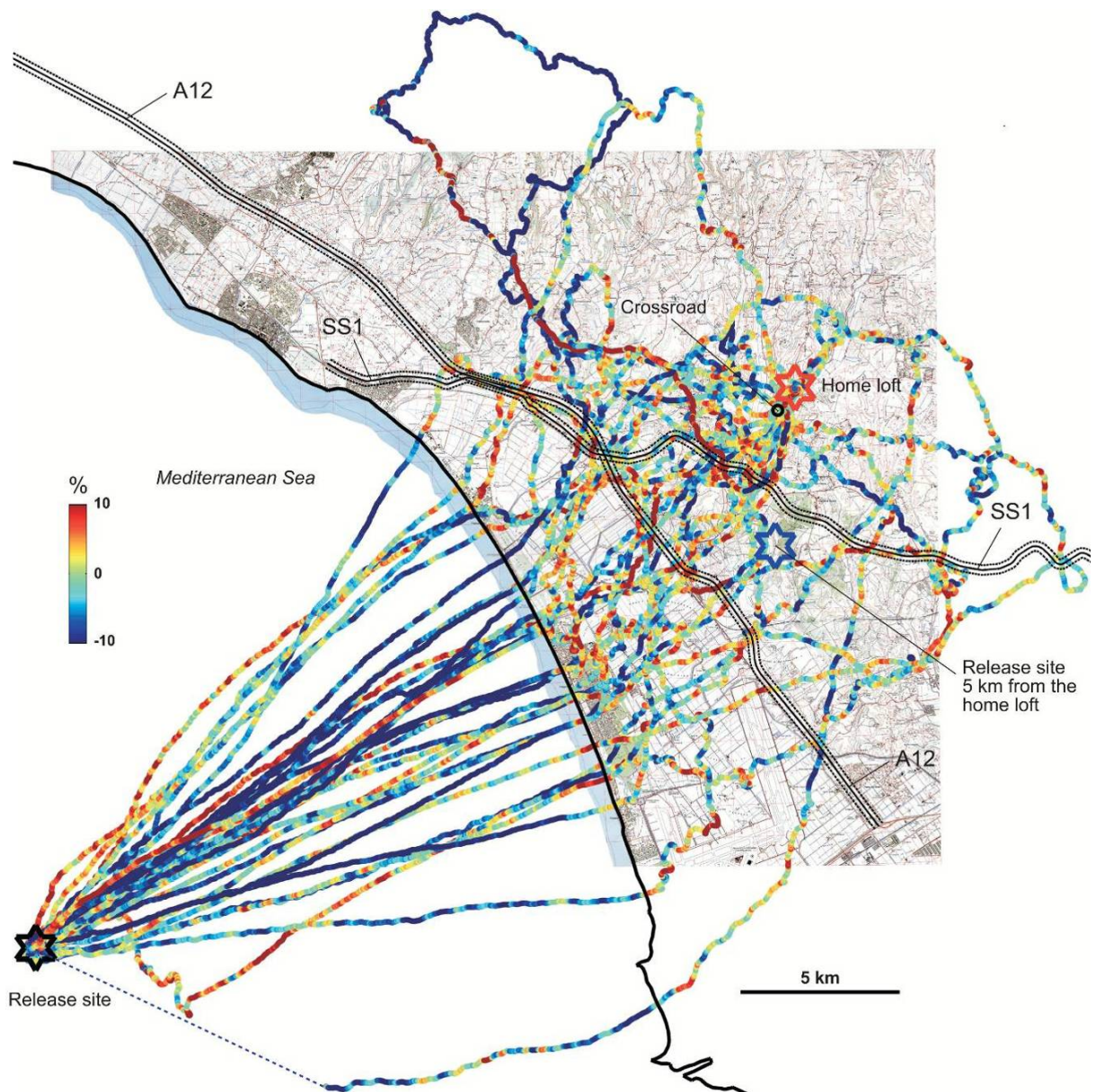
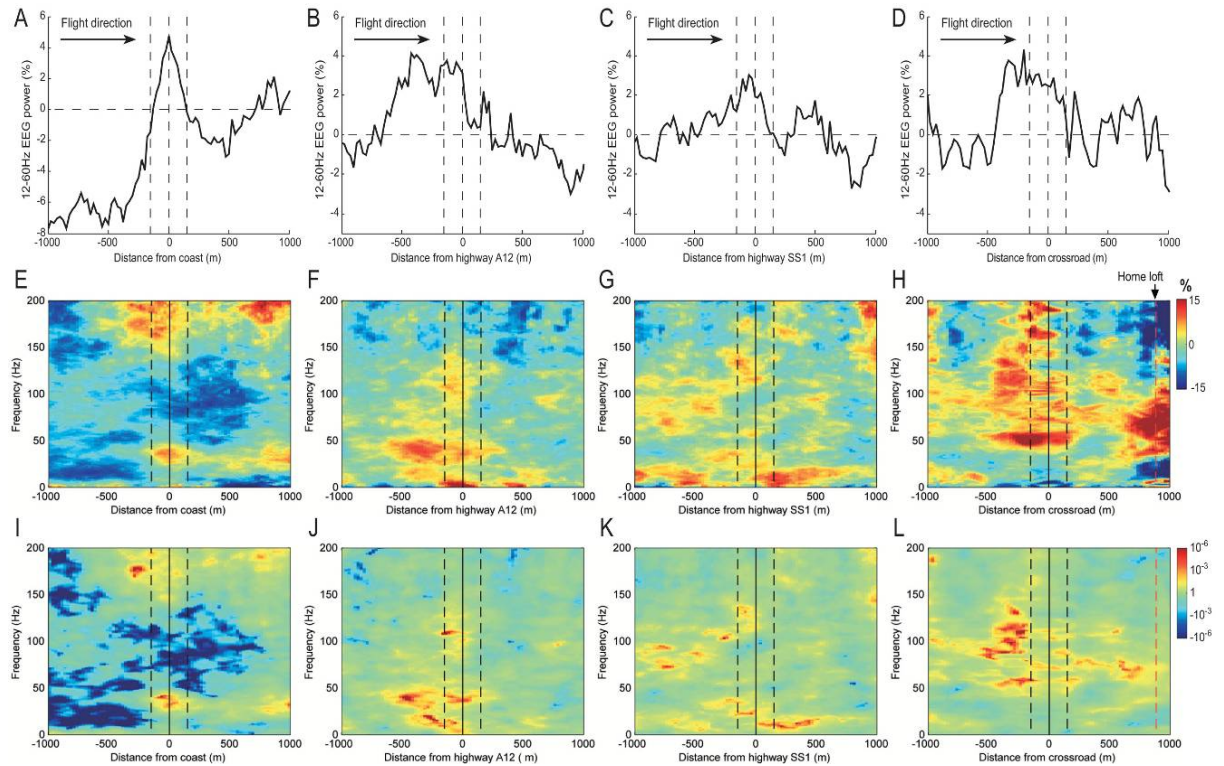


Figure S9. **Color coded tracks of all three sea releases plotted together.** Color shows EEG power in C range (12-60Hz, in %). Increase of power in C range over the coast and highways is notable in some tracks.



**Figure S10. 12-60Hz EEG power is increased in pigeons flying over well-visible ground objects such as coastal line, highways A12 and SS1, and crossroad.** (A - D) Dynamics of C range (12-60 Hz) EEG power near the coast, highway A12, highway SS1 and crossroad respectively. Vertical dotted lines denote 150-m area near landmarks. (E - H) Distance-frequency (DF) representation of EEG power (in %). (I - L) DF representation of probability (two sided  $t$ -test,  $N = 33, 33, 32$  and  $17$  respectively) multiplied by the sign of deviation. Note that activation of C frequency band was always associated with some activity in higher frequencies. Over the coast E band (130-200 Hz) was activated, and over other landmarks – D band (60-130 Hz). For details of computation see Supplemental Experimental Procedures.

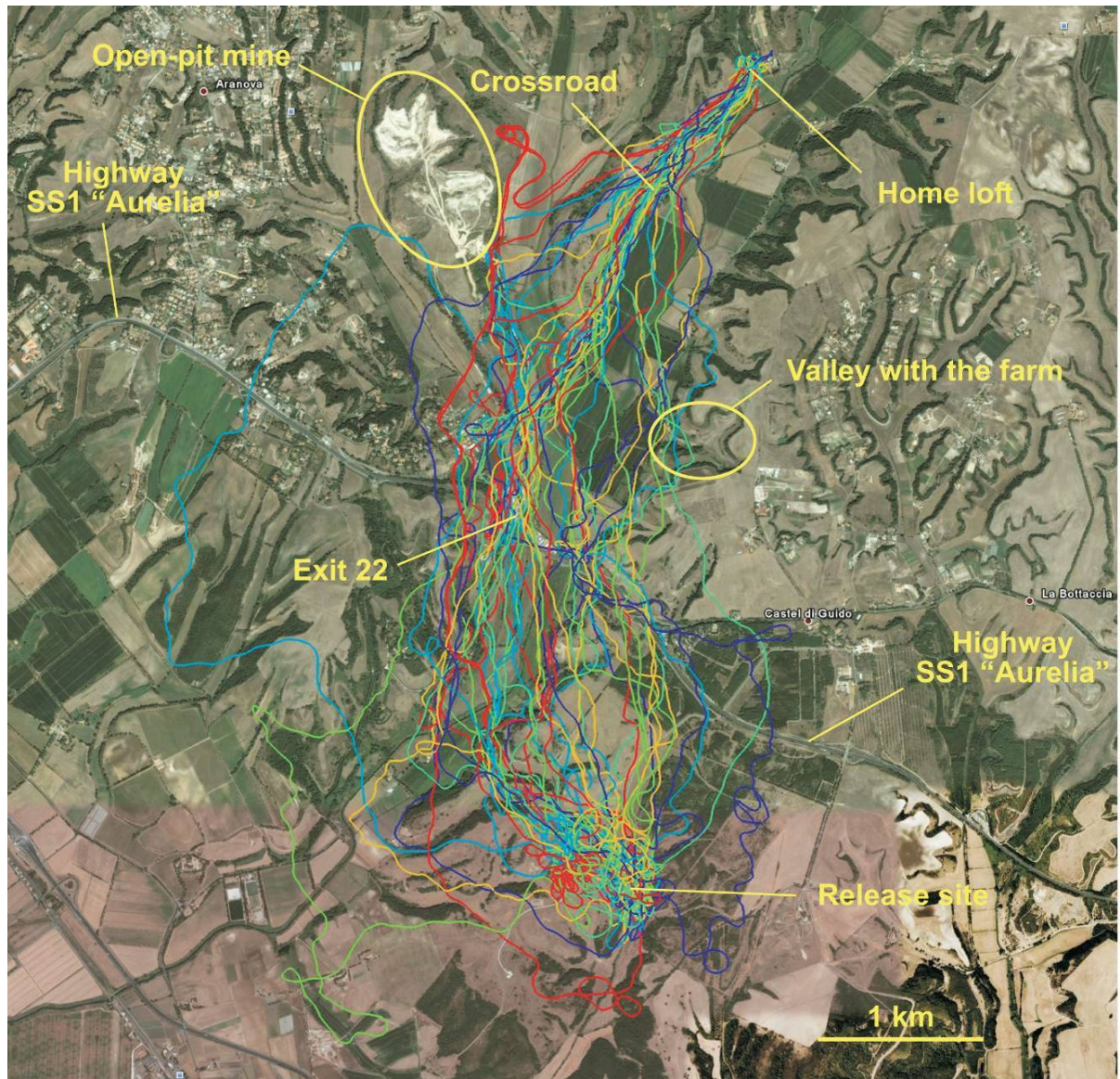


Figure S11. **Satellite photograph of area of 5-km releases.** 48 pigeon tracks are shown. Satellite image from Google Earth.

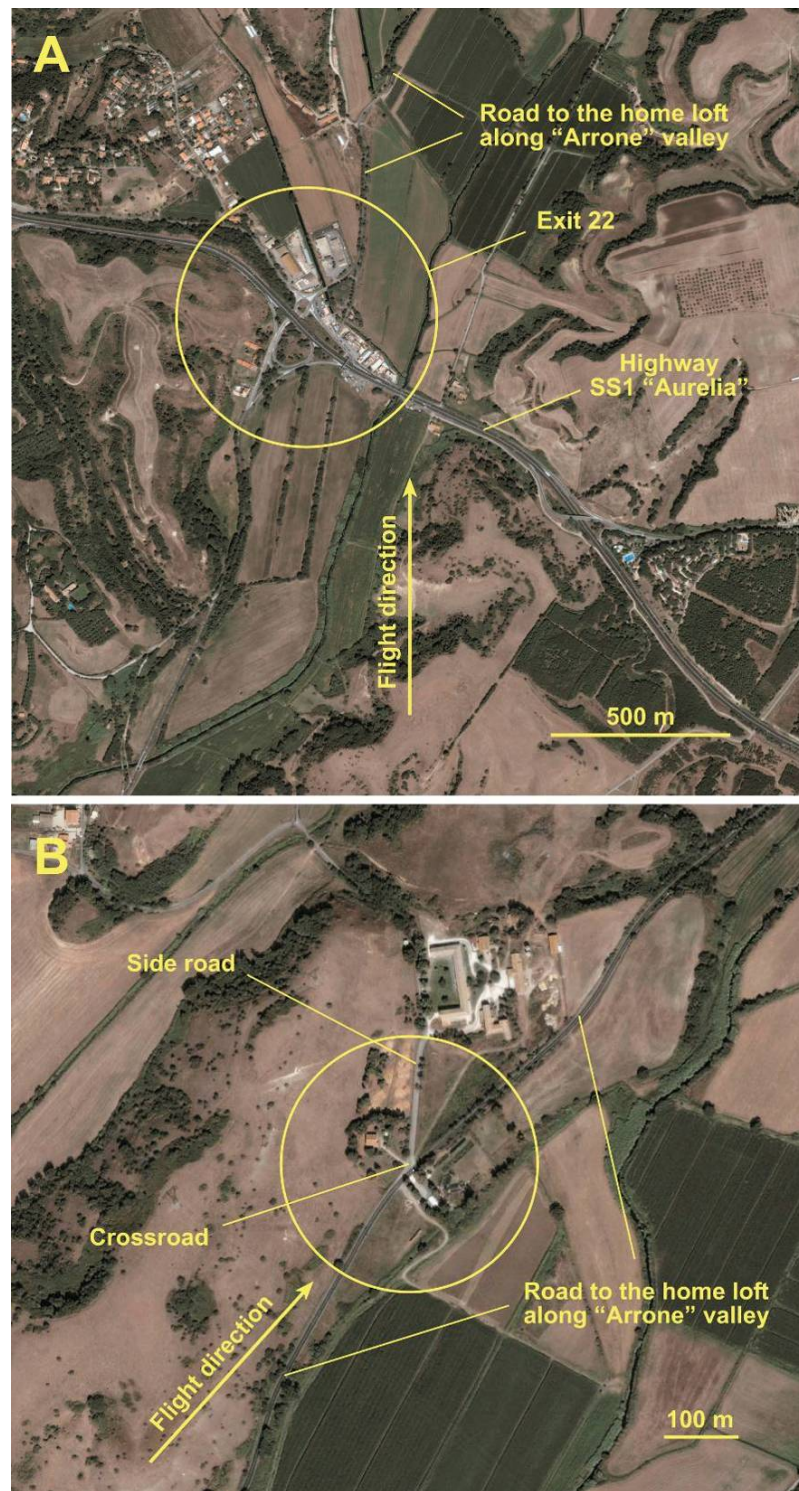


Figure S12. **Satellite views of the Arrone valley.**

(A) Exit 22 of the highway SS1 “Aurelia”. Pigeons approached the highway SS1 “Aurelia” from the South (indicated by the arrow) at an angle of about 30 degrees to the perpendicular line to the highway. Thus, animals saw the highway first by the right eye and then by the left.

(B) Key crossing with a side road. The side road with the associated infrastructures (the junction is indicated by the circle, the side road goes up from its center) was located on the left side of the pigeons’ path indicated by arrow. A colony of feral pigeons was observed there. The activation of EEG in C and E frequency bands mainly in the right hemisphere reflects visual perception of ethologically relevant stimuli on the left side. Satellite images are taken from Google Earth.

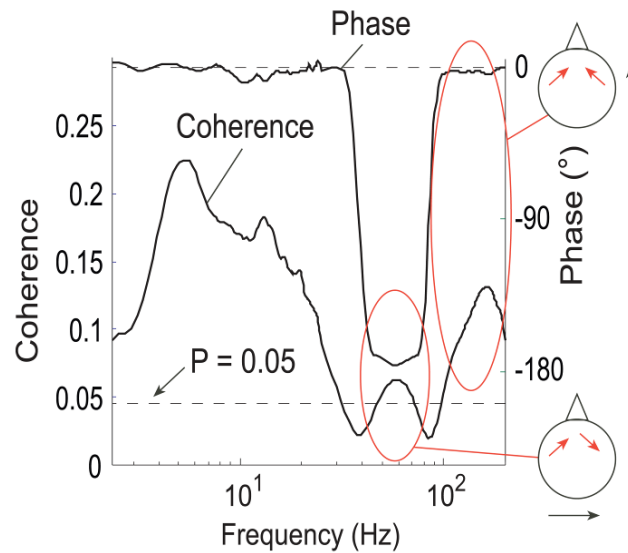
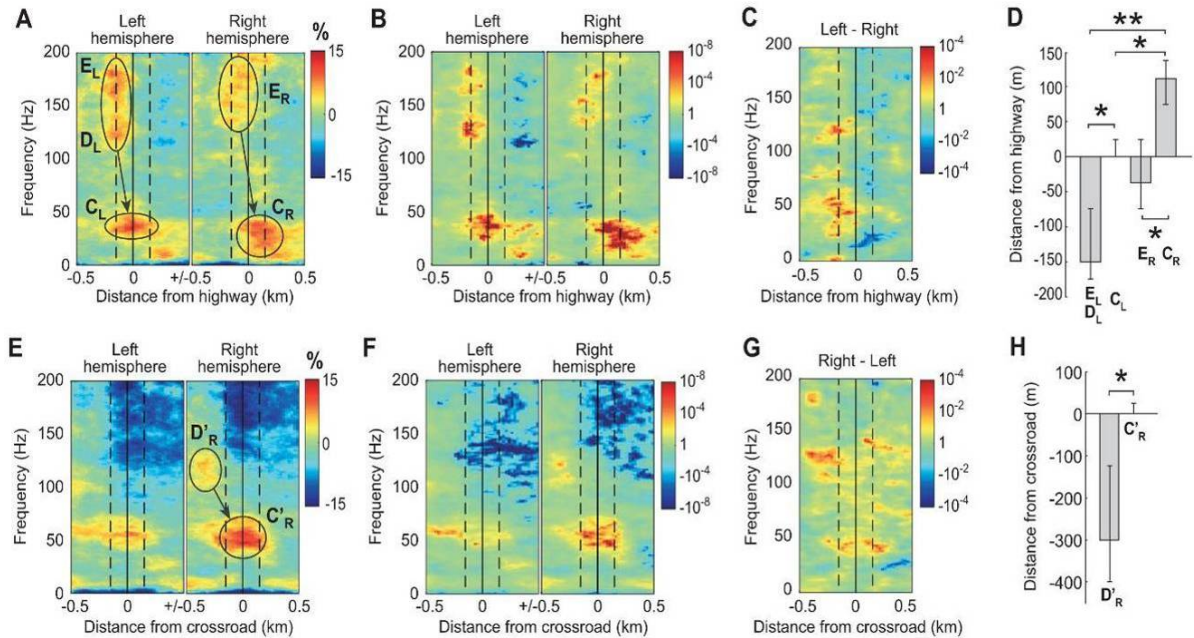


Figure S13. **Interhemispheric coherence and phase difference.** Interhemispheric coherence corresponds to the left scale and phase difference  $\varphi(\text{right}) - \varphi(\text{left})$  – to the right scale. These parameters do not depend on bird location. The dominant directions of oscillations are shown by arrows on schematic pigeon head drawings. The direction of arrows indicates direction of the field vector at one moment. This vector oscillates along this axes with a frequency indicated at the horizontal axis and in the next half of a period the direction will be the opposite. The lower dotted line indicates the value of coherence 0.044 at which the significance of coherence  $P = 0.05$  is reached (for the current duration of dataset 1h 18min). If coherence exceeds this level, it is statistically significant. The dataset for coherence computation was formed by taking every 10<sup>th</sup> epoch from the pool of all artifact-free epochs of 5-km releases.



**Figure S14. Asymmetrical activation of hemispheres in the vicinity of landmarks**

(A) Distance-frequency (DF) representation of EEG power near the highway. The direction of flight is from the left to the right as in the previous figure. Zones of increased power on distance-frequency plane of particular interest are surrounded by ovals and are labeled by letters denoting frequency band (C, D, E) with the indexes L or R for the left or right hemisphere respectively. Sequential activation of these areas is indicated by arrows.

(B) DF representation of probability of deviation from the baseline near the highway.

(C) DF representation of probability of difference in EEG power between left/right hemispheres near the highway.

(D) Maximums of EEG power of zones (E<sub>L</sub>D<sub>L</sub>), E<sub>R</sub>, C<sub>L</sub> and C<sub>R</sub> relative to the highway location. Error bars show quartiles for the medians. Asterisk,  $P = 0.05$ ; two asterisks,  $P = 0.001$  (bootstrap, 22 birds). High frequencies (E, D ranges) were activated before medium frequencies (C range) in both hemispheres. In C frequency band the left hemisphere was activated before the right (C<sub>L</sub> – C<sub>R</sub>,  $P < 0.05$ ). In high frequencies ((E<sub>L</sub>D<sub>L</sub>) – E<sub>R</sub>) a similar tendency was observed.

(E-H) Activation of hemispheres near the crossroad, similar to (A-D), zones of increased EEG power are labeled as D'<sub>R</sub> and C'<sub>R</sub>.

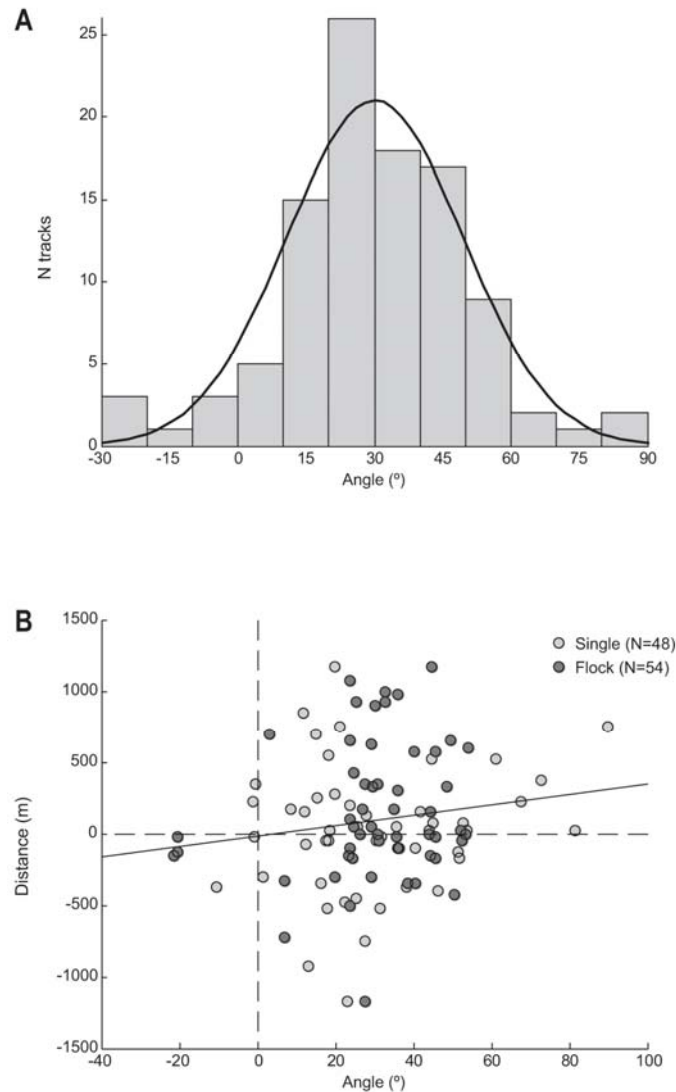


**Figure S15. Dependence of interhemispheric delay of C band activation on the angle between highway SS1 and pigeon trajectory in 5-km releases.** Angle is calculated from the perpendicular line to the highway. (A) Distribution of angles at which animal tracks crossed the highway ( $N = 102$ , track of single and in flock flying pigeons are pooled). Smooth line represents fitted normal distribution curve. (B) Correlation of interhemispheric delay with angle. Interhemispheric delay is calculated as distance in meters between two maximums of activity in the left and in the right hemisphere respectively. Positive correlation means that when, for instance, the road is visible first from the right side, the left hemisphere is activated before the right. Pearson correlation  $r = 0.150$ ,  $P = 0.133$ ,  $N = 102$ .

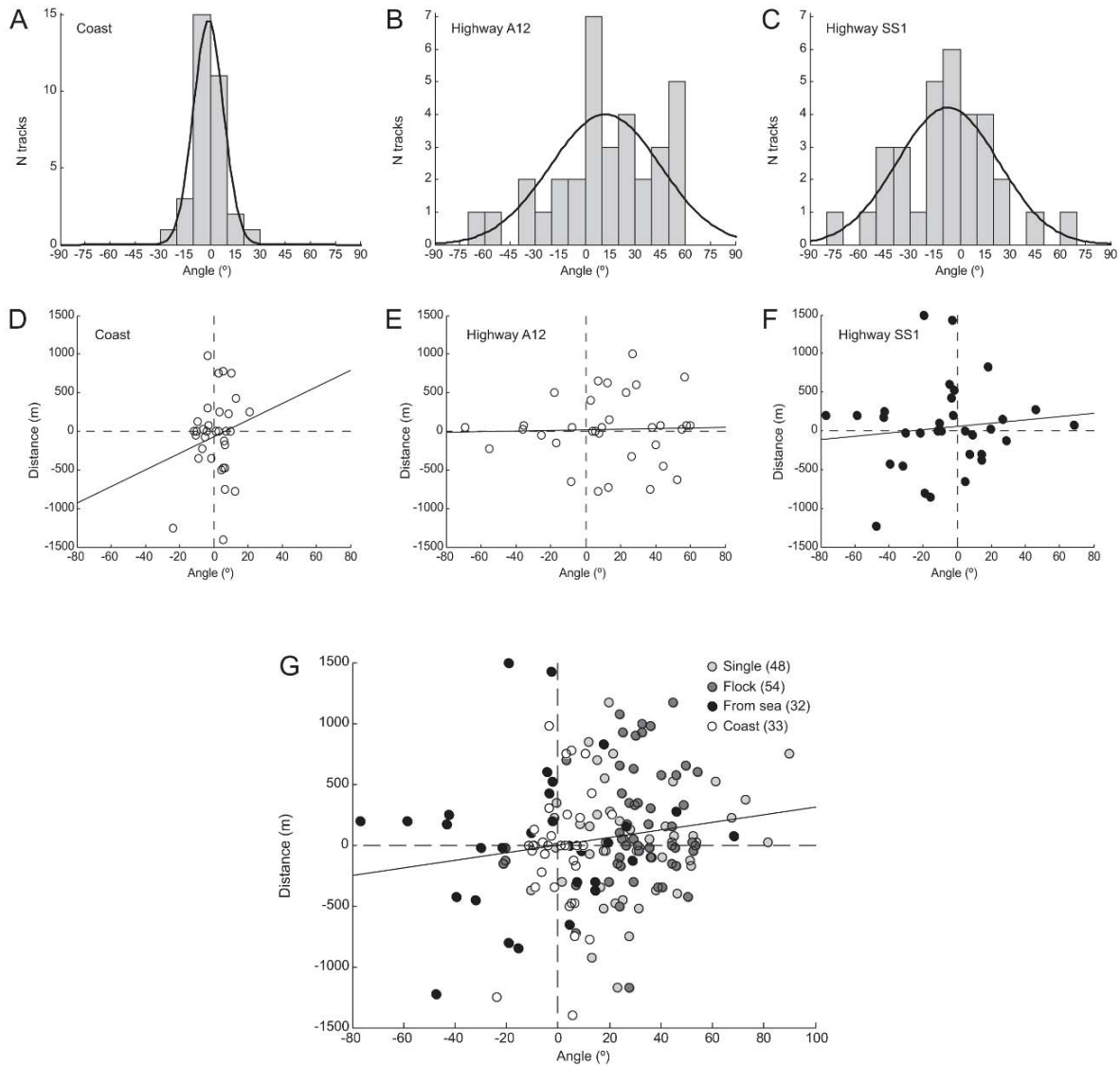


**Figure S16. Dependence of interhemispheric delay of C band activation on the angle between longitudinal landmarks and pigeon trajectory in releases from sea.** Angle is calculated from the perpendicular line to the landmarks (coast, highway A12 and highway SS1). (A – C) Distribution of angles at the coast, highway A12 and highway SS1 respectively. (D - F) Correlation of interhemispheric delay with angle at the coast, highway A12 and highway SS1. Correlation and significance: Coast -  $r = 0.184$ ,  $P = 0.304$ ; Highway A12 -  $r = 0.026$ ,  $P = 0.884$ ; Highway SS1 -  $r = 0.116$ ,  $P = 0.529$ . (G) Correlation of interhemispheric delay with angle for pooled data (over coast and highway SS1, for 5-km releases and releases from sea). Correlation is significant ( $r = 0.162$ ,  $P = 0.037$ ,  $N = 167$ ).

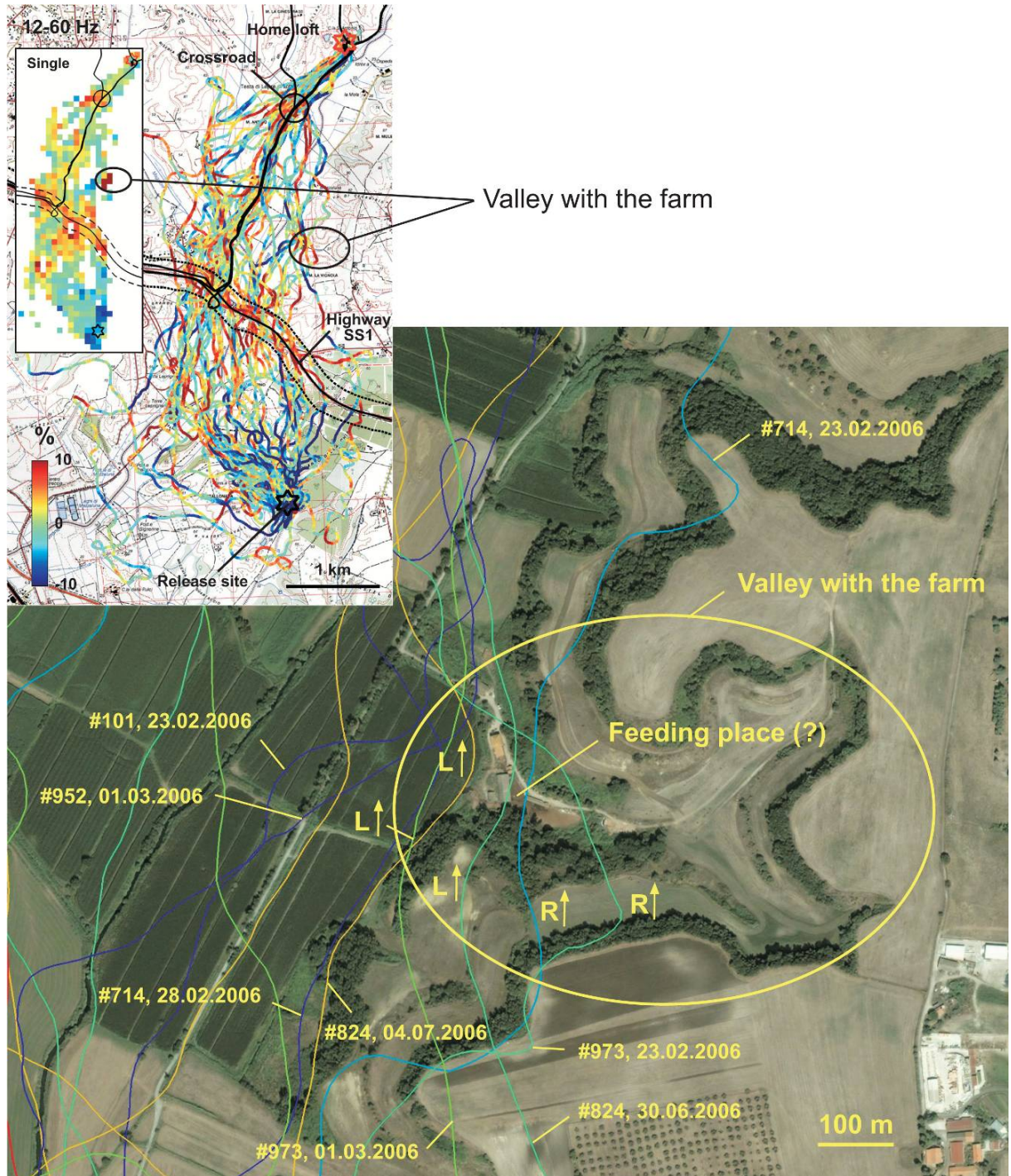


Figure S17. **Satellite view of small valley with farm.** Inset shows color-coded C band (12-60Hz) activity along tracks in birds flying along (Figure 3A). Pigeons passing the area labeled “Feeding place (?)” at left had predominantly left-hemispheric activation (L↑) in C frequency band (12-60Hz), as they saw object with the right eye. Pigeons passing the potential feeding place at right had right-hemispheric activation (R↑). Pigeon tracks are labeled with pigeon’s numbers and dates of releases. Pigeons #714, #824 and #973 appeared to have developed an affinity to this place as they passed over this valley more than once. Later we observed a colony of feral pigeons there. Satellite image from Google Earth.

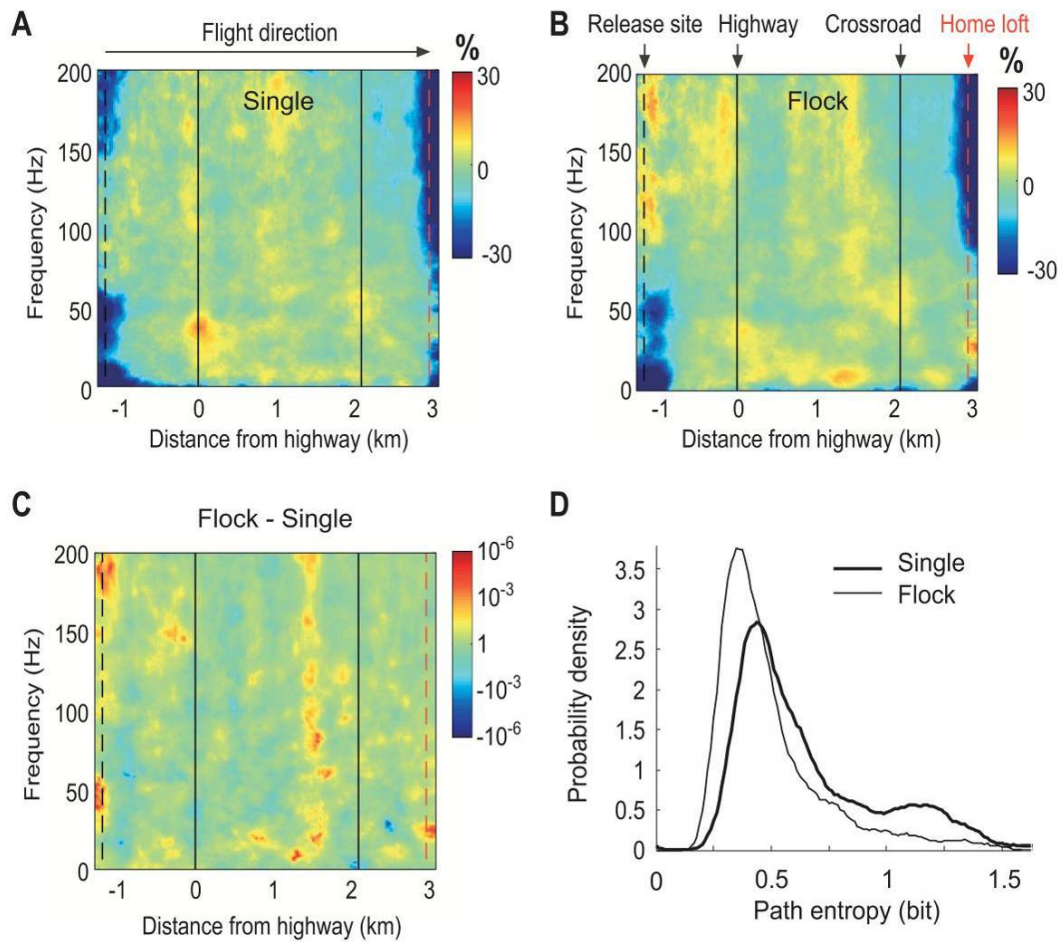


Figure S18. **EEG power at the release site and near the home loft is increased in flocks, but not in birds flying alone.** (A) Distance-Frequency (DF) representation of EEG power of pigeons flying alone. (B) DF representation of EEG power of birds flying in flock. (C) DF representation of probability of difference in EEG power between birds flying in flock and alone. (D) Probability density of path entropy. See Supplemental Results for additional description and comments.

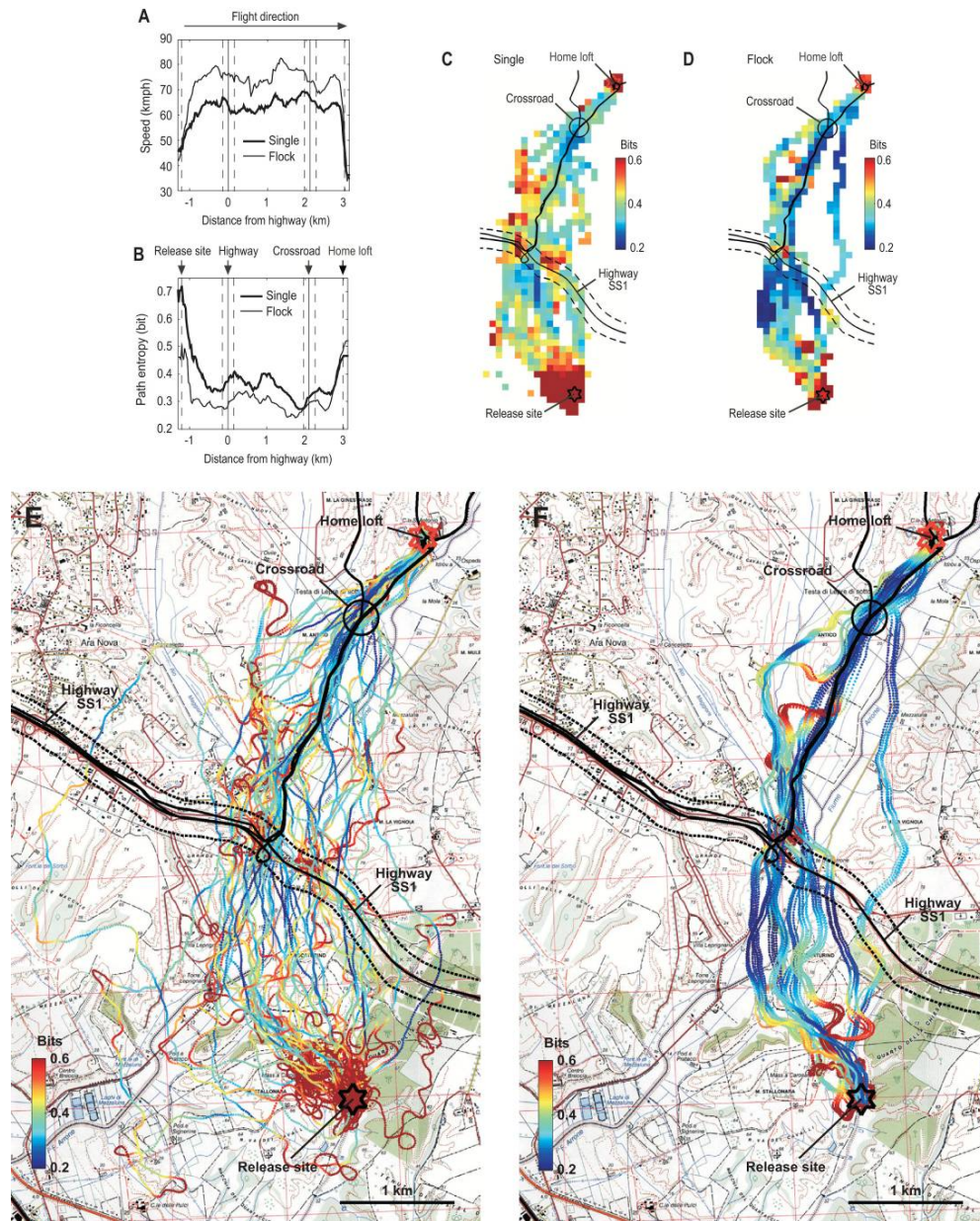


Figure S19. **Changes in flight behavior in the vicinity of the landmarks**

(A) Flight speed. (B) Path entropy.

Average flight speed of flocks are higher, than birds flying singly ( $75 \pm 8$  kmph vs.  $63 \pm 7$  kmph, mean  $\pm$  s.d.,  $P = 3.3 \cdot 10^{-4}$ ,  $N_1 = 48$ ,  $N_2 = 10$ , Mann-Whitney), and path entropy is smaller ( $0.33 \pm 0.06$  bit vs.  $0.40 \pm 0.08$  bit,  $P = 9.8 \cdot 10^{-3}$ ,  $N_1 = 48$ ,  $N_2 = 10$ , Mann-Whitney). However, flocks and singles undergo similar changes in speed and path entropy while flying over highways and crossroads: speed decreased and path entropy increased by an approximately equal extent in these groups (difference is N.S.). (C, D) Path entropy in pigeons flying alone (C) and in flocks (D) averaged in  $100 \times 100$  m squares. Please note that spatial profile of entropy differs from spatial profile of EEG power in C frequency range (insets in Figures 4A and 4B). Contrary to EEG, entropy is not increased homogeneously over highway SS1. Instead of this, two dark brown spots indicating high entropy are observed near highway. (E, F) Path entropy along individual tracks of pigeons flying alone (E) and in flocks (F). Trajectories of pigeons in flocks were slightly (several dozen meters) shifted from each other in the horizontal direction to show color of each track (in this and other similar pictures). The mean coordinate of the flock was kept unchanged. In reality animals were flying mostly in very compact flocks with a distance of several meters in between. But had data been plotted in this way, only one color-coded trajectory would be visible for each flock.

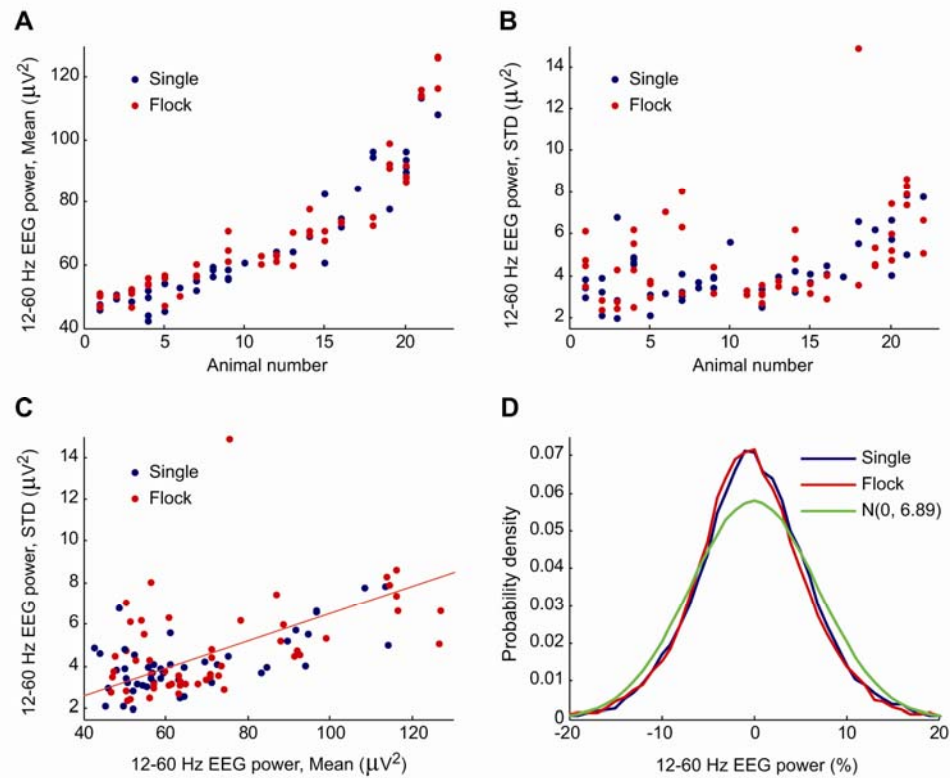


Figure S20. **Statistical properties of 12-60Hz EEG power in the flight.** (A) Average values for individual releases. Animals ( $N = 22$ ) are sorted in ascending order by their average 12-60Hz EEG power. Number of single releases – 48 (blue bullets), number of tracks of flock releases – 54 (red bullets). (B) Standard deviation (STD) of 15-sec episodes from the mean of each release. (C) Correlation of STD in the release with the average power of the release. The red line is a regression line passing through the point (0, 0). (D) The distribution of the power in 15-sec episodes expressed in percents of the average power. The green curve is a normal approximation of distributions of single and flock tracks taken together ( $\sigma = 6.89\%$ ).

## Supplemental Results

### *Unilateral visual stimulation cause marked asymmetry in the pigeon's EEG, whereas the intrinsic functional brain asymmetry has only moderate impact*

The EEG from 17 pigeons was recorded in four conditions: – with both eyes open, with the left eye occluded, with the right eye occluded, and with both eyes occluded. EEG spectra recorded from the left and the right hemispheres with both eyes open (normal condition) did not differ (Figure S3A). Fourier transformation was applied using 2-sec, artifact-free epochs. Thus, the frequency bins follow each other with 0.5 Hz intervals. The procedure for rejecting the artifact-contaminated epochs is explained in the Supplemental Experimental Procedures. EEG power between the left and the right hemispheres differed by less than 7% over the whole frequency range (Figure S3B). Percentages were calculated relative to the mean power of both spectra at the selected frequency. Red lines indicate standard deviation of the mean. Thus, the EEG power of the left and right hemispheres deviate less than one sigma from each other at all frequencies. This shows that there was no hemispheric asymmetry when both eyes were open. Therefore, this condition is referred to as the “baseline state”. Subsequently, percentage deviations from this baseline state were calculated for each animal separately and then averaged to produce charts (Figures S3C-S3E). Occlusion of both eyes caused an increase of EEG power in frequency bands A, B, and D (see Figures S3F for frequency band definitions), and a decrease in frequency bands C and E in both hemispheres (Figures S3C, S3D). Changes were in the same direction in both hemispheres, but the increase of power in frequency band B in the left hemisphere was somewhat larger than in the right (Figure S3E). Interestingly, occlusion of the contralateral eye caused almost the same shift in EEG spectrum as occlusion of both (Figures S3C, S3D). Occlusion of the ipsilateral eye caused much smaller changes (Figures S3C, S3D). Such a strong influence of the visual input on the EEG power spectrum of the opposite hemisphere implies that visual input is a determinant factor of pigeon EEG. Figures S3F, S3G and S3H represent the significance of deviations represented in Figures S3C, S3D and S3E respectively. Figures S3F and S3G show the two-tailed  $t$ -test probability of deviations from the baseline state multiplied by the sign of the deviation. The 0.05 probability boundaries are labeled by red dotted lines. It should be noted that the probabilities shown in the chart are constructed by the moving average, and do not represent probabilities of separate bins across the Fourier spectrum. Figure S3H shows the two-tailed  $t$ -test probability of deviations of asymmetry (Figure S3E) from zero - constructed in the same way. Although the largest deviation in percent power is observed in the B frequency band, the most significant deviations

were observed in high frequencies – in the C, D and E bands. Coherence of the EEG with the neck electromyogram in the frequency bands A and B suggests that the increased variance in these frequency bands was due to penetration of low-frequency muscle activity in the brain. Therefore, high-frequency bands C, D, and E may represent the state of the avian brain more reliably than the often used low-frequency activity. Hemispheric asymmetry in reaction to visual input was significant at some frequencies (Figure S3H), indicating moderate functional asymmetries. The asymmetrical position of the ground electrode cannot account for this, because potentials in the left and right hemispheres were taken relatively to corresponding reference electrodes placed symmetrically. Also, EEG spectra recorded from the left and the right hemispheres with both eyes open (normal condition) did not differ (Figure S3A).

### ***EEG in A and B frequency ranges is coherent with the neck electromyogram***

Why is the difference in high frequencies C, D, E between different physiological states more statistically significant than in low frequencies A and B? We suggest that the low statistical significance of the ranges A and B may be caused by artifacts caused by electrical muscle activity in the neck. This hypothesis was tested by recording an electromyogram (EMG) from the neck muscles simultaneously with EEG in the flying pigeon. Myographic electrodes were implanted subcutaneously to pick up local muscular activity. The dependence of EEG-EMG coherence on frequency is shown in Figure S5A. For comparison, we also recorded EEG and EMG in pigeons under the following conditions: (i) resting in a grid cage with a view of the environment outdoors, (ii) resting with both eyes occluded by eye-caps, and (iii) while sleeping.

Statistically significant EEG-EMG coherence occurred in flying pigeons in the 3.5-11 Hz range, and in sitting pigeons with open eyes in the 1-7.5 Hz range. In the first of these two cases, coherence achieved a maximal value of 0.2, in the second – 0.1. EEG-EMG coherence levels did not reach significance in either the pigeon sitting with occluded eyes nor in the sleeping pigeon. If the magnitude of observed variations lies in a range of 5-10% of the average value of EEG power, this means that EEG recordings in low frequencies (<12 Hz) can be easily confounded by the muscle activity in the flying bird. This is likely one of the reasons why low-frequency avian EEG in flying pigeons is not very informative. Interestingly, there was also an almost significant EEG-EMG coherence in high frequencies (>80 Hz) in the flying bird (Figure S5A) for which we have no explanation.

Similarly, one can note that EMG (Figure S5B) and EEG (Figure S5C) spectra do not show increase around frequencies at which EEG-EMG coherence is high. During flight, EMG power is approximately 10 times higher (equally over the whole spectrum) than in the sitting bird (Figure S5B). During sleep, EMG power is approximately 10 times lower than in a resting awake pigeon in both low (<3 Hz) and high (>100 Hz) frequencies. A peak near 9 Hz in pigeons that had either both occluded eyes or were sleeping is probably produced by a tonic discharging of the posture-maintaining muscles. In cats, such bursts have been observed with a frequency of 6-12 Hz [29].

The most interesting conclusion from this EEG-EMG analysis is that avian EEG appears quite robust to artifacts at frequencies between 20-80 Hz, in spite of the relatively minor variance in this range. This suggests that oscillations at these frequencies may be important for avian brain functioning.

The value of the scaling exponent in pigeon is close to 2, which is the theoretical value for Brownian noise that is random at longer intervals, but is easily predicted and strongly correlated at short lags [13]. A scaling exponent close to 2 is typical for electrocorticograms in mammals in the gamma frequency range [30, 31].

***EEG power in C and D frequency ranges depends on visibility/experience, while EEG power in E frequency range does not depend on them***

Color-coded EEG power of the C range along trajectories of pigeons in three sequential releases from sea is shown in Figure S6. In some tracks (plotted as red continuous lines) EEG was not recorded for technical reasons. Horizontal visibility (haziness) during all these releases was different. In accordance with the record of the nearby Fiumicino airport weather station (see Figure S6), the mean visibility was 8.2, 6.0 and 10.3 km, respectively, but all releases took place under a sky that was sparsely to moderately clouded. These measurements coincide with visual estimation of visibility by experimenters at the release site and with animal flight behavior. On the day of the first release (Figure S6A), the direction of flight of pigeons over the sea showed high variability, most probably because this was the first sea release after several months.

On the second release day, when visibility was rather poor, pigeons appeared to head for the shortest distance to the shore (Figure S6B), possibly because they were unable to distinguish prominent visual features of the coastline. Records of the weather station showed

that wind directions could not account for this deviation from the beeline. Under these conditions of reduced visibility, the behavior during and after release indicated that the pigeons had orientation problems. They were circling for prolonged periods around the boat, and some pigeons tried to land on the boat repeatedly and had to be chased away. One bird even jumped back into the start cage after release.

On the day of the last release visibility was unusually good and all animals flew directly to the home loft, close to the beeline (Figure S6C).

During all three releases the average speed of the flight over land did not differ ( $69.6 \pm 3.7$ ,  $71.8 \pm 5.2$ ,  $68.8 \pm 5.1$  km/h, mean  $\pm$  s.d.,  $P_{12} = 0.30$ ,  $P_{13} = 0.73$ ,  $P_{23} = 0.16$ ; only values from birds with good EEG were taken:  $N_1 = 8$ ,  $N_2 = 12$ ,  $N_3 = 13$ , non-paired two-tailed  $t$ -test, Figure S7A). This indicates that animals were in similar physical condition and had similar motivation to fly home over ground on these three days. However, flight speeds across the sea were different: on the first day it was  $63.4 \pm 9.2$  km/h, on the second and third  $80.9 \pm 3.6$  and  $74.0 \pm 3.2$  km/h respectively. All these values differ significantly from each other ( $P_{12} = 1.20 \cdot 10^{-5}$ ,  $P_{13} = 1.20 \cdot 10^{-3}$ ,  $P_{23} = 1.20 \cdot 10^{-5}$ ,  $N_1 = 8$ ,  $N_2 = 12$ ,  $N_3 = 13$ , non-paired two-tailed  $t$ -test, Figure S7A). The relatively slow speed during the first release might indicate a novelty effect, while the high speed under poor visibility might reflect the tendency to reach the shore as fast as possible.

In spite of different conditions no differences in altitude of the flight or in path entropy between the releases were found (Figures S7B and S7C). Path entropy is a measure of uncertainty and stochasticity within a trajectory ([24], see also Supplemental Experimental Procedures). The maximum altitude of about 110 m was reached 6 km after release, and decreased thereafter to 50-70 m. Over land the pigeons maintained this altitude relative to the ground (Figures S7B). The path entropy was high (0.5-0.7 bits) at the release site and home loft (reflecting circling paths over these places), moderate over land (0.4 bits), and low over sea with a slight decline from 0.3 to 0.2 bits from release site to the coast (Figures S7C).

The dynamics of EEG power in frequency ranges C, D and E are presented in Figure S8. The red line presenting EEG power in the third release with good visibility differs notably from the green and blue lines representing EEG power in the first and second releases in the Figures S8A and S8B. No differences between releases were observed for the EEG power in the frequency range E over sea (Figure S8C).

*Changes in EEG power do not occur synchronously in both hemispheres*

The many trajectories from the 5-km release site permitted exploration of whether the landmark crossed elicited changes in the EEG bands specifically upon activation through the left or the right eye, assuming that the pigeons oriented their heads predominantly in the direction of flight. Since the pigeon's fields of vision of the left and right eye are overlapping for only a limited frontal area, differential hemispheric EEG activation in specific bands might help to identify special features of interest. Thus, we undertook an exploratory analysis of the coherence of oscillations occurring in the left and right hemisphere [25]. In case of strong coherence, we expected to detect synchronized processing, while low coherence would indicate independent hemispheric processing.

Estimation of coherence showed that these oscillations were strongly coherent in the low-frequency ranges A and B (below 30 Hz, Figure S13), but much less (albeit still statistically significantly) synchronized in frequency ranges C and E during the whole flight (Figure S13, coherence reaches values 0.23 at 5.5 Hz, 0.063 at 60 Hz and 0.13 at 160 Hz, 2-sec epochs,  $N = 1998$ , significance level  $P = 0.05$  is 0.044, bootstrap). Such low coherence values indicate that high-frequency activity in these bands measured unilaterally originated predominantly from local sources in the same hemisphere and these sources were not synchronized with sources of oscillations in the opposite hemisphere.

Separate analysis of activity in the hemispheres confirmed this hypothesis. When approaching the highway, activation of the brain started with the high-frequency activity (areas  $E_L D_L$  and  $E_R$ , Figure S14A, letters E, D and C denote frequency bands as earlier) in both hemispheres (the apparent delay of the right hemisphere activation comparatively to the left was not statistically significant,  $P = 0.22$ ). Activation of high frequencies is followed by activation of medium frequencies in both hemispheres (areas  $C_L$  and  $C_R$  at Figure S14A, respectively). Activation of these frequencies is significantly delayed in both hemispheres relative to ipsilateral high frequencies activation ( $P = 0.031$  and  $P = 0.035$  for the left and right hemispheres, respectively, Figure S14D). The right hemisphere (area  $C_R$ ) was activated after the left (area  $C_L$ ) in the intermediate (12-60 Hz) frequency range ( $P = 0.049$ , bootstrap, Figures S14A and S14D).

Observed asymmetry in EEG can be explained by asymmetrical visual input: most of the birds saw the highway first with the right eye, and only later with the left eye (Figure 4 and Figures S11, S12A), because they approached it at a ca. 30° angle. Pigeons have panoramic vision arising from laterally placed eyes (with 120° between optic axes and only 37° wide area of binocular vision in front of the bird [32]) and therefore objects from the right side can be seen exclusively by the right eye, and from the left – by the left eye. However, the influence of intrinsic asymmetry of the avian brain [33, 34] can not be excluded. When flying over the crossroad (Figure 4A,B and Figure S12B), activation of EEG also was asymmetrical: the right hemisphere was activated more strongly than the left (Figures 14E, 14F and 14G). Delay in activation of the middle frequencies in the right hemisphere was significant ( $P = 0.045$ , bootstrap, Figure 14H). Such asymmetrical activation can also be caused by asymmetry in visual input: the side road and set of buildings around it were probably seen by the left eye in most birds (Figure S12B). According to this logic, the delay between left and right-hemispheric activation will be longer if the track hits the highway with a flat angle and absent if the track hits the highway orthogonally. We calculated the angle of crossing for each track interpolating the path direction from 250 m before the highway (distance to midline crossing, not orthogonally measured) and 250 m after it and correlated this angle with the onset delay between left and right hemispheres. In birds flying alone and in flocks the average angle of highway crossing (calculated from the perpendicular to the highway) was similar:  $29.8 \pm 21.9^\circ$  for singles,  $30.3 \pm 17.0^\circ$  for flocks and  $30.1 \pm 19.4^\circ$  for all tracks together (mean  $\pm$  s.d.). Deviations of angles assumed a normal distribution (Figure S15A). As predicted, interhemispheric delay has a tendency to correlate positively with the angle between the track and the perpendicular to the highway at crossing point (Pearson correlation  $r = 0.147$  for birds flying along,  $r = 0.155$  for flocks and  $r = 0.150$  for all together, figure S15B). The line of linear regression  $y = 3.644 \cdot x - 14.85$  ( $y$  – in meters,  $x$  – in grads) passes very close to the point (0, 0) and predicts that in case of crossing the highway orthogonally, one can expect simultaneous activation of both hemispheres. However, because of high variability of data, correlations are not significant ( $P = 0.318$ ,  $P = 0.262$  and  $P = 0.133$ , for singles, flocks and all tracks together respectively). To clarify whether dependence of interhemispheric delay on the angle is coincidental or not, we analyzed in the same way intersections of tracks of sea releases (Figure 2) with longitudinal landmarks such as coast and highways A12 and SS1. Distributions of angles and corresponding correlation plots are presented in Figures S16A-S16F. Here we can see the expected correlation by the coast and by the highway SS1. However, it was absent by the highway A12. The most probable explanation of this phenomenon is that a set of significant landmarks lies just before the highway A12 on the pigeon's way. Before the northern part of

highway A12 (the upper part of Figure 2), highway SS1 lies just several hundred meters before it. Additionally, a railway goes in parallel to A12 and pigeons have to cross it before crossing the highway (it looks like a thin dark smooth line between highways and the coast, just 150 meters before highways in some places, Figure 2). In the previous study [11] it has been shown that this railway also can serve as a guiding line for homing pigeons. Influence of additional landmarks on EEG activation over highway A12 is visible also from Figures S10B, S10J, where two peaks of C band activation are observed: one is about 500-400 meters, and another 150-0 meters before the highway. Because of identical tendencies we pooled the data from different longitudinal landmarks to calculate average dependence of interhemispheric delay on the angle (Figure S16G). Here we draw the regression line  $y = 3.100 \cdot x - 0.436$  that occurred very close to the previous estimation based on highway SS1 and 5-km releases only. Pearson correlation  $r = 0.162$  was significant in this case ( $P = 0.037$ ), showing that dependence of interhemispheric delay on the angle is not coincidental. However, to get statistical significance we had to pool 167 samples. And if we add the data from highway A12, excluded earlier for reasons explained above, we shall get Pearson correlation  $r = 0.138$  and probability  $P = 0.0517$ . Here we would like to stress, that a weak dependence does not mean that the phenomenon described is meaningless biologically. It just shows that C band oscillations can be affected by other visual cues and maybe by other factors, uncontrollable under conditions of free flight.

***EEG power at the release site and near the home loft is increased in flocks, but not in birds flying alone***

Distance-Frequency (DF) representation of EEG power of pigeons flying alone and in flock is shown in Figures S18A and S18B. Note the similarity in the middle parts of these charts. However, at the release site and home loft (labeled by dotted lines) EEG power of birds flying in flock is higher, than in birds flying alone. This is indicated by orange-red areas at frequencies of 100-200 Hz at the release site and around frequencies of 20-30Hz near the home loft. A comparison of these groups shows that the EEG power just near the release site in the frequency intervals 45-55 and 150-200 Hz was significantly higher when pigeons were flying in a flock ( $P \sim 10^{-5}$ , Figure S18C). A divergence of such degree was not observed between these groups at other places. Such activation may reflect social interactions at the start, when birds form the flock. At arrival, EEG power also increased in flock birds, but in the another frequency range - 20-30 Hz ( $P \sim 10^{-5}$ ). Here, the birds have to split from the flock and decide in which loft they should go, as flocks were formed from pigeons belonging to different lofts and this process may

be reflected as activation of EEG. The distribution of path entropy was clearly bimodal in single animals (Figure S18D). Bimodality of distribution indicates two discrete states [24]. The state with the high-entropy occurs mainly when pigeons released alone circle near the release site – a well-known behavior typical for pigeons. Pigeons released in flocks demonstrate such behavior to a much lower extent. Many have hypothesized that birds acquire some navigation-relevant information during this circling behavior [12]. As it can be seen from Figure S18A, however, there is no visible activation of EEG near the release site in pigeons flying alone, instead, there is even some decrease in EEG power. This suggests that such behavior is not linked with activation of visual attention in birds.

### *Alternations in EEG over landmarks are accompanied by changes in flight behavior*

Analysis of the flight dynamics derived from GPS tracks of homing pigeons can be used to identify objects of interest for pigeons. This is not only evidenced by circling or directed approaches, but also by more subtle parameters such as changes in flight speed, altitude, flight tortuosity and path entropy [24]. Thus, these parameters were analyzed with respect to a possible relationship with the EEG and the particular landmarks characterizing the short-distance terrestrial releases.

In general, speed decreased when birds were flying over relevant landmarks (Figure S19A). The difference in speed 150 m before and after a landmark was significant (landmarks: highway and crossroad taken together  $P = 3 \cdot 10^{-5}$ , highway  $P = 1.4 \cdot 10^{-2}$ , crossroad  $P < 10^{-5}$ , bootstrap). Altitude decreased over the landmarks (highway and crossroad  $P = 1.3 \cdot 10^{-4}$ , highway  $P = 5.5 \cdot 10^{-4}$ , crossroad  $P = 2.3 \cdot 10^{-3}$ , bootstrap). However, this coincides with a general trend of altitude reduction from the release site to the loft, as the place of release was 25 m higher relative to the home loft. A small increase in path tortuosity was also observed, yet due to its high variability, this tendency was not observed over highways (highway and crossroad  $P = 1.0 \cdot 10^{-3}$ , highway  $P = 0.12$ , crossroad  $P = 4.2 \cdot 10^{-4}$ , bootstrap). Flight entropy increased over the landmarks (Figure S19B, highway and crossroad  $P = 2.6 \cdot 10^{-3}$ , highway  $P = 4.7 \cdot 10^{-2}$ , crossroad  $P = 9.4 \cdot 10^{-3}$ , bootstrap). On the other hand, there were clear dissociations between path entropy and EEG variations as evidenced by comparing single and flock-flying birds (Figures S19C-S19F).

## Supplemental Experimental Procedures

**Neurologger electronics.** The second generation of the neurologger device, also called Neurologger 2 to distinguish it from the previous version [15], was used in the current study. The electronics of the 17.5x14.5 mm printed circuit board (PCB) of the Neurologger was powered by two ZA10 1.4 V zinc-air batteries (Renata Ltd.). The PCB incorporated front-end amplification (2000x) and filtering, a 16-bit MSP430 microcontroller (Texas Instruments Corp.) running at 4.4 MHz, and 256 MB of non-volatile memory. The microcontroller had a built-in 10-bit, 8-channel, 200 ksps ADC. The circuitry was powered by a 2.0 V voltage regulator. The technical data of the Neurologger is summarized in Supplemental Table 1. Additional information can be found at <http://www.vyssotski.ch/neurologger2>. A photograph of the Neurologger and its attachment with the GPS logger to the pigeon are presented in Figure S1. The microcontroller was programmed in assembler. A custom USB adapter was used for connection of the Neurologger with a PC running Windows. A utility for communication with the Neurologger was written in Delphi 7.0 (Borland Corp.). The logger utilized analog high- and low-pass filters of the first order that have attenuation of -20 dB per decade with a quite oblique attenuation profile near the cut-offs (-3 dB). Thus, the frequencies near the borders were also recorded, but with moderate attenuation. This allowed, despite the non-optimal 1-70 Hz range, the recording of 70-200 Hz frequencies with sufficient quality. Moreover, these high frequencies that were artificially attenuated by the filter were back-compensated by software during the analysis. All spectra were corrected in this way. The signal was digitized by the microcontroller with a sampling rate of 1600 Hz. Means of sequential groups of four samples were stored in the non-volatile memory with a rate of 400 Hz for further analysis. The sampling frequency was derived from the on-board quartz with a precision of +/-30 ppm. Thus, the maximal possible time drift in the Neurologger does not exceed 12.96 sec in 5 days. In practice, the drift was even smaller – 8.53 sec in 5 days on average. As the duration of the experiments did not exceed a few hours, the drift of the internal clock of the Neurologger was negligible. Logger's performance has been validated in experiments on mammals [16].

**Surgery.** Gold-covered watch screws were used for epidural EEG recording. The procedure of their implantation is described in a previous publication [15]. They were placed according to stereotaxic coordinates as given by Karten and Hodos [35] (Figure S2): ground electrode – AP2.5, L2.0 (in the left hemisphere), left/right reference electrodes – AP5.0, L±5.5, left/right signal electrodes – AP8.5, L±2.0. Positions of electrodes were chosen to pick up signals from the brain regions participating in processing of visual information (visual wulst) and cognition

(*nidopallium caudolaterale*). The position of the ground electrode is not important when there are separate reference electrodes, because voltage is measured relatively to the reference. Additionally, two electrodes were implanted in the dorsal part over the *cerebellum* with coordinates AP-1.0, L $\pm$ 3.5. Signals from the cerebellar electrodes were not used in the current analysis due to their stronger coherency with the electromyogram (EMG) as compared to rostral electrodes. Such signals are difficult to interpret since they represent a mixture of brain oscillations and muscular activity. In one pigeon, in addition to the electrodes described above, two electrodes (Cooner Wire AS633,  $L = 20$  mm with the last 5 mm free from the insulation) were implanted in the neck subcutaneously, symmetrically, and dorsally for EMG recording.

**Behavioral experiments.** All experimental manipulations with the birds started after a 4-day post-operation recovery period. The research was conducted between February and July 2006.

Experiments with birds in cages. The influence of eye occlusion on EEG was investigated by placing the birds ( $N = 17$ ) singly in an outdoor cage (43x30x32 cm). Pigeons were allowed to observe the surrounding environment and the EEG recording started after a 20-min adaptation to the cage. The pigeon vision was manipulated in a sequence of four conditions: both eyes open, left eye occluded, right eye occluded, both occluded. Eyes were occluded by circular eye-cups fixed with Velcro® strips. Recording of each condition lasted 20 minutes. The whole sequence of four conditions was repeated twice, without a break, for a total time of 160 min recording and the EEGs corresponding to the same condition were pooled together as no difference in power was observed between them. EEG in sleep was recorded in four pigeons kept singly, in the same cages, in a dark, sound-proof room during the night from 20:00 to 08:00. It is known that pigeons placed in darkness soon fall a sleep [36], and 93% of that sleep is slow-wave sleep (SWS) [37]. We analyzed one-hour period EEG from 01:00 to 02:00. During this interval slow wave patterns were clearly dominant.

Experiments with flying birds. Between releases, birds always wore PVC dummies of the same weight as the GPS in order to habituate them to the load. The total load did not exceed 30 g, which corresponds to a daily portion of food picked up and carried in the crop – it is thus a physiological load typical for foraging pigeons. For experiments, the dummies were replaced with GPS-loggers (Newbehavior, Zurich, Switzerland; Technosmart, Rome, Italy) just before the release, and placed again on the bird after retrieving the GPS at the loft. The ground-based release place was located about 5 km to the South of the home loft (4.913 km S, 0.612 km W, Figure 2). All animals ( $N = 22$ ) were familiarized with the area by regular training to home from different locations before the surgery. Additionally, before starting the experimental

releases on land, the birds were released twice from the experimental release place to control for possible loss of performance due to the surgical procedure and for additional familiarization with the territory. Pigeons were transported to the release site by car in a well-ventilated, visually-shielded transport cage.

For sea releases, 16 pigeons were trained, prior to surgery but carrying GPS dummies, to return from a maritime location about 18 km from the coast (17.278 km S, 23.557 km N from the home loft, Figure 2). After operation, they were released three times with an interval of one week. For technical reasons, not all records were suitable for analysis. Complete EEG-GPS records of good quality were obtained in 8, 12 and 13 flights, respectively. Pigeons were transported to this site by boat in shielded transport crates. Prior to release, GPS-loggers and neurologgers were activated, and the birds placed individually in a small releasing crate permitting scanning of the environment. They were not tossed but allowed to leave the crate after opening of the cover. This helped to estimate the flight motivation of the pigeon.

## Data analysis

### *Purification of the datasets before statistical analysis*

EEG records usually contain episodes of abnormalities caused by muscle activity and by other sources from outside of the brain. The existence of such episodes in the dataset increases variance and decreases robustness of the statistics. For this reason we removed such episodes from the dataset. To do this, we split the continuous EEG record into epochs and removed those containing artifacts according to our criteria (see later). For the analysis, where a high resolution of the EEG dynamics seemed to be important (i.e. during flight), we used epochs of one second, which coincided with the 1Hz sampling of coordinates by the GPS. In sleeping and sitting pigeons, and for comparing spectra of the flight over sea and land, we used 2-sec epochs.

The artifact-rejection procedures were applied to the intervals of interest only, mainly to reduce the computational work, as these procedures are computation-intensive. Thus, for the flights, in order to remove episodes of sitting, take off and landing, we took only epochs at time points where pigeon speed exceeded 30 km/h. In the experiments with eye occlusion, in which the comparison between states was important, the whole set of episodes (8x20 min) was filtered as a single block to avoid possible biases, as thresholds of some rejection procedures depend on variance (and other statistics) of the dataset.

The epochs containing artifacts were rejected by the tools included in the EEGLAB package [25]: finding of abnormal values (threshold  $\pm 200 \mu\text{V}$ ), finding improbable data (5 SDs), finding abnormal distributions (5 SDs), and finding abnormal spectra ( $\pm 50 \text{ dB}$  in range 20-80 Hz). This procedure yielded an acceptable percentage of rejected data in all cases ( $< 10\%$ ).

After rejection of artifact-contaminated epochs, the power spectrum was calculated for each remaining epoch by Fourier transformation.

For flight periods, it was necessary to preserve the precise timing of epochs for synchronization with the spatial coordinates. To do this, the power spectra of rejected epochs were replaced with the values obtained by linear interpolation of the nearest good preceding epoch and the following epoch.

#### *Equalizing within track variation*

Preliminary analyses showed that EEG power varied largely between individual pigeons (mean EEG power in 12-60 Hz frequency band of individual pigeon tracks is given in Figure S20A). Significantly different values of EEG power in different birds (varied from  $48.6 \mu\text{V}^2$  to  $119.5 \mu\text{V}^2$ , the span is  $70.9 \mu\text{V}^2$ , mean  $\pm$  s.d. =  $69.6 \pm 20.2 \mu\text{V}^2$ ) could be explained in part by variations in the electrode implantation between individuals. Mean power varied much less between different releases of the same bird (the maximal span is  $23.9 \mu\text{V}^2$ , s.d. =  $4.17 \mu\text{V}^2$ ), and is comparable with the variability within flight (Figure S20B). EEG power in the 12-60 Hz frequency band did not differ between birds released alone and in flock ( $P = 0.13$ , bootstrap,  $N = 22$ , non-parametric, ranks were counted separately for different birds). The average standard deviation of power of 15-sec intervals within a flight was  $4.51 \mu\text{V}^2$ , the maximal -  $8.63 \mu\text{V}^2$ , excluding one outlier of  $14.89 \mu\text{V}^2$ . The dependence of the Standard Deviation of the trajectory from its mean power was plotted (Figure S20C). Dots have a notable tendency to aggregate around a regression line drawn through the point (0, 0) – indicating linear proportionality between mean power of the release and standard deviation of power of episodes during the release. In order to minimize the influence of the variability discussed above and increase the power of the statistics, the power of epochs (the power of each epoch) was standardized by dividing it by the average power of the trajectory. The distribution of standardized power of 15-sec episodes was seen to be symmetrical with a shape very close to the normal distribution with  $\sigma = 6.89\%$  (Figure S20D). In spite of similarity with the normal distribution in general shape,

the distribution of EEG power has heavier “tails”, i.e. positive kurtosis and should be classified as a supergaussian distribution [38]. In our case, the distribution can be easily normalized by truncating outliers producing the “tails” (specifying an appropriate truncation threshold), or by a normalizing transformation. Normalization was not necessary, as our distribution was very close to normal, and values of probabilities obtained with and without normalization were very similar.

We also equalized influence of different frequencies by calculating the power in the frequency ranges as weighted mean. In fact, the EEG power spectrum has a strong decline from low to high frequencies. Thus, the sum of power of the frequencies in the range of 12-60 Hz will have a dominant influence of low frequencies, which eventually could mask differences in other frequencies of the range. Splitting one wide frequency range into several smaller ones may be questioned as arbitrary classification. To equalize the influence of such different frequencies on power estimation, we decided to pool the power of frequency bins with weights inversely proportional to the power of these bins. We found that the flight EEG power spectrum can be approximated, on average, by the equation  $P(f) = A/f^\alpha$ , where  $P$  – power density in  $\mu\text{V}^2/\text{Hz}$ , constant  $A = 100$ ,  $f$  – frequency in Hz, and the “scaling exponent” [13]  $\alpha = 1.74$ . Thus, weights were chosen  $\sim f^\alpha$ , with the normalizing coefficients making the average of the weights equal to 1, to get power in  $\mu\text{V}^2$ . The idea behind such weighting is that the deviations in power at different frequencies are easier to compare when they are expressed in %, and not in  $\mu\text{V}^2$ . The power of all frequency bands in the article was calculated as described above, including in Figure S20.

### *Spatial discretization*

Data recorded by loggers represent EEG power measured at a sequence of points (X, Y) at 1-sec intervals. Such representation is inconvenient for evaluation of influence of landmarks on EEG and statistical comparison of individuals, as different tracks contain different number of points at different locations. Supposing EEG to be associated with distance from key landmarks we projected the two-dimensional coordinates to a one-dimensional scale. For each point, we calculated the distance to the landmark in 2-D (i.e. to the coast, highways or to the crossroad), and then placed this point on a one-dimensional scale with the coordinate equal to calculated distance (Figures 3A-3C, 4C, 4D, 4F, 4G and some others). Since all tracks of 5-km releases passed close to the crossroad (Figure 4), we plotted for demonstration purposes only a function of distance to the road and marked the distance from the crossroad to the highway at these

charts (Figures 4F-4G and Figures S18A-S18B). If the pigeon was approaching the landmark from the side of release, the distance was assigned a negative value, after crossing it, the distance became positive. Thus, all points to the South from the highway were labeled “minus”, and all to the North – with “plus”. All tracks after the crossroad continued straightforward to the loft (Figure 4). Through the crossroad we draw a line, perpendicular to the segment from the crossroad to the loft. To the points located South from this line (below it) we assigned “minus”, to the points from the other side – “plus”. Afterwards we calculated average EEG power for each track over 25-meter segments, following one after another counting from the landmark. If no points occurred in some segment (usually this occurred near the crossroad, as some animals bypassed it at a distance exceeding 25 meters), values obtained by linear interpolation were used. Thus, each track was characterized by a vector of EEG power relative to distances of ...-50, -25, 0, 25, 50... m from the landmark. Such discretization was used for plotting color-coded charts and for calculating statistics. However, the mean EEG power in  $\pm 150$  m areas near the landmarks was calculated as a mean of good epochs without additional discretization by 25-m segments.

### *Smoothing*

In most cases, the EEG power of 1-sec epochs along pigeon tracks showed considerable variation. In order to provide a better representation on charts, EEG power of sequential 1-sec epochs was smoothed by a moving average with a span of 15 sec. This span achieves smoothing that allows good visualization of the influence of landmarks while significantly diminishing noise in the data. Such smoothing also was applied to the flight parameters represented in Figure S19, to make them consistent with the EEG data.

Two-dimensional color-coded charts (Figures 3A,B, Figures 4F,G, Figures S10E-L, Figures S14A-C,E-G, and Figures S18A-C) were smoothed by a 2-D rotationally symmetric Gaussian filter with  $\sigma_1 = 100$  m, span 500 m,  $\sigma_2 = 4$  Hz, span 20 Hz.

Data from each track were smoothed separately before statistical analysis. Thus, mean, median and statistical significance were all calculated using the smoothed data.

The charts showing dependencies on frequency in logarithmic scale (excluding charts of coherence – Figure S5A and Figure S13) were smoothed by moving average with a span ( $\Delta f = 1 + 0.5 \cdot \text{round}(f/5)$ ), where  $f$  is frequency (Hz) at the points where the power is estimated. The

step in frequency was 0.5 Hz at these charts. Such a formula was used to provide a power spectrum in logarithmic scale: to smooth low frequencies with a small span ( $\Delta f = 1$  Hz at  $f = 0$  Hz) and to smooth high frequencies with a large span ( $\Delta f = 21$  Hz at  $f = 200$  Hz).

#### *Choice of statistics*

EEG power has a symmetrical probability density function (Figure S20D), for which median and mean coincide. Thus, both these statistics can be used for the description of the datasets. However, the power of the associated tests differs. For small datasets ( $N \leq 17$ ), tests based on sample average are slightly more powerful than those based on median scores (i.e., they give smaller probability values). However, when the size of the dataset was larger ( $N \geq 44$ ), the median became more reliable than the mean, because outliers in the heavy “tails” of the supergaussian distribution destabilized the estimate of the mean (compared to a normal distribution). Therefore, we used mean-based statistics for the small datasets (Figures 1, 5 and Figure S3), and median-based ones – for large data sets (all other figures).

#### *Choice of statistical tests*

In simple cases of balanced experimental design when each animal was tested only once, standard non-paired *t*-tests were used for comparisons. Such data were generated by experiments with eye occlusion, sleep and three releases over sea, with the numbers of animals used 17, 4 and (8, 12, 13) respectively (Figures 1, 2 and Figure S3). Paired *t*-tests were used when appropriate (Figure S14D).

In the second set of experiments aimed at investigating the influence of landmarks on EEG, pigeons ( $N=22$ ) were released multiple times. For technical reasons the design was unbalanced: i.e. different animals were released a different number of times. The amount of successive releases varied for different birds from 1 to 8 (Figures S20A and S20B).

Averaging the values of birds released several times and pooling them with the values of birds released less frequently increases probability estimates and leads to extremely small power of the test, as average values of several releases have much smaller variance than values of separate releases.

Another way to make the experimental design balanced, suitable for simple classical statistical tests, is to treat each track as an independent sample. We found that such an approach leads to realistic estimations, similar to ones of a bootstrap simulation. This happens because the EEG of a pigeon in several sequential releases is practically independent: the variance (of

EEG power in %) between sequential releases of the same pigeon is approximately equal to the variance between several birds, showing that our procedure of equalizing of within-track variation works well. However, we preferred to adhere to the conservative position and therefore do not treat several releases of one animal as independent samples.

Therefore, we estimated the probability of differences by bootstrap simulation that allows a non-balanced setup of 22 pigeons with differing amounts of tracks each. In each bootstrap iteration we formed a set of 22 pigeons selecting them from the real set randomly with replacement, i.e. pigeons could be selected repeatedly. For the set of tracks of such a simulated dataset we calculated the median of the parameter of interest (usually – EEG power), or difference between medians of two subsets, if we wanted to compare single pigeons with flocks. The null hypotheses were that the median did not differ from zero and that two medians did not differ from each other, respectively. The number of iterations for the evaluation of the difference between singles and flocks (Figure 4E) was 10000, that allowed evaluating probability of difference directly ( $P = 0.0448$ , when the road and crossing are taken together). For plotting the color-coded image in “Distance-Frequency” coordinates, only 100 iterations were done, as such an amount was sufficient for evaluating the sample average and variance (Figures 3B, 4G, S10I-S10M, S14B, S14C, S14F, S14G and Figure S18C). The mean and variance of this sampling distribution ( $N = 100$ ) were calculated, and the probability level was estimated assuming normality of the data.

#### *Positional entropy calculation*

Entropy is the measure of stochasticity of the trajectory [24]. We estimated a stochastic complexity based on embedding space decomposition (ESD), described in details by Roberts et al. [24]. However, our procedure differed in how we represented spatial coordinates for entropy computation. The entropy of the trajectory *de facto* was calculated by Roberts et al. as a sum of the entropies of two coordinates  $X$  and  $Y$ . This approach is correct when variables are statistically independent. Such assumption for pigeon tracks is questionable. Pigeons, in general, fly with relatively regular speed, slightly varying around 60 km/h. At the same time the direction of their flight may vary a lot. In such case the entropy of the path will be mainly determined by variations in the flight direction, i.e. a function of one independent variable – the angle of the speed direction  $\alpha$ . Increments of spatial coordinates will depend on it as  $\Delta X_t = |V_t| \cdot \cos(\alpha_t) \cdot \Delta t$ ,  $\Delta Y_t = |V_t| \cdot \sin(\alpha_t) \cdot \Delta t$ , where  $|V_t|$  - almost constant speed of the pigeon,  $\alpha_t$  – angle between the speed vector  $V_t$  and  $X$  axis,  $\Delta t$  - time increment between sample positions. Index  $t$  indicates dependence on time.

One solution could be to describe the trajectory not in Cartesian coordinates ( $X, Y$ ), that are dependent, but in increments of angular coordinates, i.e. in  $|V_i|$  and  $\alpha_i$ , that should be more independent.

In the current analysis we used another approach requiring a simpler computation. We noted that spatial coordinates of a pigeon ( $X, Y$ ) can be represented as coordinate on a complex plane:  $Z = X + i \cdot Y$ . Therefore, we calculated the entropy of this complex variable exactly as it was done with two spatial coordinates by Roberts et al. [24]. Of course, the embedded matrix  $\mathbf{X}$  in ESD is complex, but the eigenvalues of  $\mathbf{X} \cdot \mathbf{X}^*$  are real, and the calculated entropy also is real. Thus, transition to the complex variable  $Z$  did not cause any problem in the interpretation. The validity of such an approach is also confirmed by computations: the entropy of complex variable  $Z$  was approximately  $\sqrt{2}$  times smaller than the sum of entropies  $X$  and  $Y$ .

#### *Coherence calculation*

Figure S5A and Figure S13 represent phase cross-coherence (or “phase-locking factor”) computed by an algorithm implemented in the EEGLAB package [25], in which spectra were obtained by wavelet transform. The plotted  $P = 0.05$  significance levels were calculated by bootstrap, again in EEGLAB. However, the  $P = 0.05$  significance level for coherence also can be approximately evaluated as  $2 \cdot \sqrt{2/T}$ , where  $T$  – duration of the record in seconds. For computation of coherence in Figure S13 every 10<sup>th</sup> epoch was taken from a set of 19934 good 2-sec epochs, as such computation is extremely memory-demanding and 10% of epochs occur sufficient for evaluation of coherence with an acceptable accuracy. Thus, duration of records in Figure S13 was 3986 sec, in Figure S5A (in sec): Flight – 456, In cage eyes opened – 2330, In cage eyes occluded – 2328, Sleep – 3600.

**Table S1.**

<i>Technical data of the Neurologger</i>		
Number of channels:		4 with 2 ref. inputs (ch1 and ch2 to ref1; ch3 and ch4 to ref2)
ADC resolution:		10 bit
Input range:		+/- 500 $\mu$ V
Neurologger mechanical dimensions (without batteries):		22x15x3 mm <sup>3</sup>
Total mechanical dimensions (Neurologger, batteries):		22x15x5 mm <sup>3</sup>
Weight of 256MB neurologger board:		0.945 g
Weight of two 80mAh Renata ZA10 batteries:		0.635 g
Weight of head connector:		0.255 g
Weight of protective cover:		0.170 g
Weight of battery connecting wires:		0.050 g
<b>Total weight:</b>		<b>2.055 g</b>
Battery life time:	EEG logger, 4 channels, 100, 200 or 400sps	1 day 9 h
	Single unit logger, 4ch x 9.6ksps	23 h
256MB memory data filling time:	4 channels, 100sps	5 days 4 h
	4 channels, 200sps	2 days 14 h
	4 channels, 400sps	1 day 7 h
	4 channels, 9.6ksps	1 h 17 min
256MB data downloading time:		26 min
Interface:	3 SPI, 2.2Mbps, converted to USB via custom adapter, power supply, one CMOS digital input for events recording (shared with SPI pin)	
Data format:		Custom

## Supplemental Discussion

### *Strengths and limits of EEG analysis in flying pigeons*

EEG analysis is, at present, the only procedure that permits economical analysis of dynamic brain activity in larger samples of freely moving pigeons. Other approaches such as functional mapping by early gene activation can only reveal averaged effects of processes during the entire flight [39]. In theory, finding place cell equivalents of spatial orientation in the flying pigeons would seem attractive, but finding such cells in animals that move uncontrollably through large spaces is extremely tedious [15].

The software tools available for EEG analysis permit decomposition of frequency bands during relatively short epochs (wavelets), which can then be matched to path segments derived from GPS tracking. However, it must be kept in mind that analysis of oscillations with different origins in the pigeon brain is not a mechanistic process that allows to identify the brain structures involved and to define the associated processes easily [13]. In fact, the analyses presented here required considerable computational efforts in order to detect the changes in the EEG related to detection of the landmarks (see Supplemental Experimental Procedures). It must be considered that homing in pigeons is a process involving different sensory modalities and is also dependent on individual alertness and motivation.

### *Low-frequency bands A and B may indicate reduced state of alertness*

Low-frequency oscillations in the range from 0-12 Hz have been mainly observed in outdoor cages during resting, and during blocking of visual input. Prior to the present study, we had assumed that navigational behavior might be associated with a pigeon equivalent of the so-called theta rhythm [40], known in rodents to be locked in a (shifting) phase with the activity of hippocampal interneurons, linked with the cells encoding the position of the animal in a defined environment [41]. However, we found little evidence for low-frequency activation during initial orientation at the release site and during changing flight directions over land, nor was it related to familiar landmarks. Technically, the regular wing flapping causing motor artifacts might have masked it, but in this case one would have expected a large representation of low-frequency oscillations during the entire flight. Given that the low EEG frequency bands in pigeons (and other birds) appear to have shifted towards slower oscillations as observed in

mammals and are poorly investigated, a realistic explanatory hypothesis at present is to take them as an indicator of a relaxed emotional state with reduced attention to external stimuli.

***EEG changes in middle-to-high frequency bands are related to visual attention of landmarks and behavior at the release site***

Our data show that middle/high-frequency oscillations can be split into three stable frequency bands **C**: 12-60, **D**: 60-130, **E**: 130-200 Hz that can be activated independently both in resting and in flying pigeons. The last frequency band is probably not limited by a border at 200 Hz, but propagates to higher frequencies, which can be studied in the future.

In resting pigeons, oscillations in all these frequency bands were modulated by visual input in a unihemispheric manner: contralateral eye occlusion caused activation of the D band, but suppressed oscillations in C and E bands. In sleeping pigeons, all these frequency bands were suppressed. In a flying bird all of them were activated relatively to the resting state.

During flight, our data show that activity in the C frequency band was a reliable indicator of visual stimulation, as the appearance of an object of interest in the visual field of an eye caused activation of the C band in the opposite hemisphere, while activity changes in the other bands appeared more variable, except for the fact that activation of D or E, or both together, usually preceded activation of the C band. The differential changes of activity in these bands in relation to release site and landmarks are shown in Table 1.

Clearly, the behavior of the C frequency band was the most consistent: it was never activated at the release sites, but peaked over prominent familiar landmarks and proved to be most useful in detecting potential objects of interest (see below). All flight data indicate that this pattern is related to selective visual attention. Remarkably, the observed sequential activation of 60-200 and 12-60 Hz frequencies is congruent with human data [42]. Selective attention in humans increases gamma-frequency activity [43, 44], followed by beta-frequency activity in the somatosensory system [45-47]. Notably, humans, performing a virtual navigation task through a maze on a computer screen, demonstrated, like our pigeons, an increase of EEG power around 38 Hz at T-shape junctions, and this increase was proportional to the duration of decision-making [48]. Consistent with animal findings, the sources of human gamma-frequency activity were identified in the primary visual cortex [49].

The D band appeared activated at most landmarks and release sites in birds flying singly, with two exceptions: it did not occur at the short-distance terrestrial release site when the birds were released singly, and it was decreased when the pigeons approached the coastline. The co-activation with the C band when approaching landmarks is in line with the finding in humans (see above), and suggests a memory reaction linked to visual perception. The decrease while approaching the coastline is difficult to interpret. It would seem that activity variations in this band are state-dependent, marking transitions between oscillatory states rather than indicating a particular activity.

The variations in activity of the E high-frequency band appear intriguing. They occurred always at the (unfamiliar) sea release sites, and were observed only over the first landmark encountered by the birds (either the coast line during sea releases, or the highway SS1 during the short distance releases) but not over subsequent ones, which clearly elicited activation of the C and D bands. The important exception from this observation is the open-pit mine. This is the single landmark (from a set of landmarks analyzed) in the vicinity of which the direction of the animal flight changed significantly. Pigeons were flying first towards this landmark having it on the left (Figures 5A and 5B). At some point they made almost a 90-degree turn to the right towards the loft. This behavior can be associated with decision-making, choosing of one from two alternatives: to fly further towards the open-pit mine and into a valley leading away, or to turn 90-degree to the loft. We hypothesize that E band activation indicates cognitive processing linked with the setting of different navigational strategies or decision-making according to a chosen strategy. Interestingly, such changes in D and E bands were not observed thus far in flock-flying pigeons passing the pit-mine. This might reflect passive orientation (following companions), but further studies identifying flock leaders and followers would be needed to confirm this hypothesis.

When released at unfamiliar sites on the sea, the present and our earlier study have shown that the birds oriented invariably to the shore, but the direction chosen can be influenced by previous training experience causing significant deviations from the beeline to the loft [50]. This indicates that pigeons released at sea relied on their ability to determine their location using their map sense based on the perception and neural integration of still debated geophysical (sun, magnetism) and olfactory information, but also relied on memory of training, and deduced from this the initial homeward compass direction when cues sufficient for the relative (to the loft) position determination were absent. The GPS tracks in this and other studies show that, once pigeons reached the coastline they deviated from their initial direction

towards a new and more correct direction leading to the loft. This process is accompanied by an increased path tortuosity which indicates increased attention to (or distraction by) landmarks. Clearly, further studies with electrodes placed in different brain structures are needed to verify whether activation of the high-frequency bands reflects the key process in pigeon navigation and homing.

Taken together, it appears that activation of the different frequency bands in the EEG activity of pigeons reflects some form of hierarchical processing: complex processes such as determining position and flight compass are associated with high-frequency oscillations, selective visual attention with middle frequencies, while activation of low frequencies appears to be associated with relaxed emotional states and species-specific behaviors.

### ***Independent hemispheric processing***

Our data from resting pigeons show that severe reductions in EEG power in several bands could be observed in the hemisphere whose corresponding eye was occluded. Since the visual input to hemispheric processing is completely crossed in pigeons [51], and interhemispheric processing takes much more time due to the lack of dedicated interhemispheric connections like mammalian *corpus callosum* [52], such a result is not too surprising but indicates that the visual inputs clearly activates oscillations in frequency bands as they were also observed during flight. Future studies must test whether the changes in the middle-to-high frequency bands represent a visual signature only, or whether similar responses might be observed after presentation of sensory cues thought to be relevant for pigeon orientation.

During flight, consistent with the in-cage study, statistically significant asymmetry of the EEG in the C frequency band was found as a response to asymmetrical visual stimulation, and not as consequence of an internal brain asymmetry. Detailed analysis of activity in D and E frequency bands during flight has shown that they also can be modulated asymmetrically by skewed visual cues (Figure S14). However, both hemispheres were activated in the vicinity of landmarks in these frequency ranges, even in case of an unilateral visual stimulation (Figure 5C), and seem to participate in the processing of navigation-relevant information.

### ***Post-hoc analysis of tracks***

An intriguing opportunity offered by this technique is to analyze individual pigeon tracks post hoc, specifically, for changes in the C band. As shown in Figures 2A and S9, variations in the

middle-frequencies occurred at many locations over land, some of which were related to the familiar landmarks SS1 and A12 (which were often used as guidelines by pigeons released along the coast from northwest (see Figures 1, 3, 5 in [11])). On the other hand, C band activation occurred at familiar places where we did not expect it, for example, when passing a crossroad fairly close to the loft (which turned out to harbor a feral pigeon colony). On the other hand, it is also clear that changes in the C band occurred in different locations, sometimes associated with changes in the flight trajectory, sometimes without distinct directional changes. Flying pigeons always scan their aerial environment, this being most evident when they spot other flying pigeons and join them. In addition, they must look out for predators and scan the ground for close or distant objects of ecological or navigational relevance. Our data show clearly that the oscillation state in the C band corresponds to selective attention, be this to familiar objects like landmarks, to locations populated with other pigeons, or to other unknown objects or stimuli encountered during flight. This is a remarkable finding – the constant stream of visual information entering a pigeon’s brain might also have masked specific events triggering visual attention.

Whatever the physiological origin of C band variations might be, our data show that it is possible, at least to some extent, to “read” a pigeon’s mind during its journey home by means of EEG analysis. Demonstration of this phenomenon was possible because we could analyze several tracks of birds passing over or in vicinity of relevant (from a pigeon point of view) landmarks. The color-coded flight tracks show that episodes of C band activation were not frequent. However, their detection could allow a selection of locations for a detailed analysis, not only of EEG and topography, but also of associated subtle geometrical changes in GPS tracks such as path entropy. Since analysis of GPS tracks is more economic than decomposition of spatially distributed EEG, there is hope to validate and extract relevant parameters indicating selective attention of pigeons during flight from GPS tracks. Lastly, it remains to be determined, by means of laboratory and outdoor studies, whether the middle- and high-frequency variations in EEG are exclusively visually dependent, or whether they might also provide a signature for olfactory and magnetic stimuli thought to guide pigeon navigation. The results reported here offer some hope for this.

In principle, the approach used here is not limited to pigeons but can be used for many other species, provided the necessary equipment can be placed and data retrieved. Ongoing technical progress in miniaturization and telemetry renders this perspective realistic.

### ***Possible brain structure origins of the oscillatory activity***

The potential candidates for the generation of such brain activity should possess two properties: they should be involved in the processing of visual information or navigation and should produce synchronized oscillatory activity. Additional requirements are that these structures should not be too small and should not lie too deep inside the brain, as high-frequency oscillations are highly attenuated - owing to volume conduction in tissues [53]. Unfortunately, our knowledge about high-frequency oscillations in the avian brain structures is extremely limited. Recordings from the *optic tectum*, the largest structure involved in visual processing in birds (see Figure S2), have shown oscillations of both local field potential and multiunit activity at frequencies of 20-50 Hz [54-56], and also fast oscillatory bursts (500-600 Hz) [57]. Synchronicity of neuronal discharges also has been found in the *nidopallium caudolaterale* (NCL) – a structure suggested to be analogous to the mammalian *prefrontal cortex* [27]. The NCL is known to be involved in higher cognitive processes such as working memory [58, 59], choice behaviour [60], organization of action sequences and reversal learning [61], and even decision making [62]. Anatomical studies have shown that the NCL receives input from all sensory association areas [63]. In spite of quite intensive investigations, no large-scale neuronal synchronicity, or oscillatory activity has been found in the pigeon *hippocampus* [40, 64]. This raises the possibility that mechanisms of synchronized oscillatory activity in the avian hippocampal formation may be somewhat different from that in rats, where a large-scale synchrony was found in three frequency bands: theta (4-10 Hz), gamma (30-80 Hz), and fast oscillations (80-200 Hz) [13]. However, the principle role of the hippocampus in avian spatial cognition is well-established now [65-69].

Existence of oscillations in the pigeon *visual wulst* may be predicted from the experiments on turtles, in whose cortex visually induced electrical waves were shown [70]. Gamma oscillations are known to be generated in the olfactory bulbs of pigeons, but this electrical activity does not propagate to the *cerebrum* [71]. Oscillations also may come from the *cerebellum*, whose oscillatory activity (usually in range 8-25 Hz) has been shown in humans [72] and monkeys [73, 74]. Faster oscillations (30-260Hz) have been discovered in the *cerebellum* of mice and rats recently [75-77]. Alternatively, it could be that high-frequency oscillations come from outside the brain, for instance, being generated by the ocular movement. Although this possibility cannot be completely excluded, there are several considerations which make such an explanation unlikely. First, ocular artifacts in birds have large amplitude and specific shape [78] compared to EEG. Epochs containing such artifacts were easy to reject by

artifact-filtration procedure [15] (see also Supplemental Experimental Procedures). As a stimulated eye moves more, it also should produce more artifacts, i.e. an increase of the oscillatory activity should be observed ipsilaterally, and not contralaterally, as it was in our experiment (Figures 1, 5, S3 and S4).

There is also a further explanation in addition to the hypotheses discussed above. As strong, large-scale oscillations were found in the *optic tectum*, and other areas do not possess large lamellar structures (with the exception of *cerebellum*) suitable for generating oscillations, it is likely that source of oscillations is the *optic tectum*. The *optic tectum* is a large structure of the avian brain with 15 cellular layers [19]. Its parts are functionally different, and vary a lot in low-frequency potentials [79]. Therefore, it cannot be excluded that signals recorded from electrodes were generated by different regions of *optic tectum*. This hypothesis does not mean, however, that the *optic tectum* also undertakes the information processing. It rather suggests that activity of different brain regions may be reflected somehow in the tectal oscillations. The *optic tectum* not only sends signals to areas of higher information processing, but also receives reciprocal projections from some of them [63]. Similarly to the mammalian *prefrontal cortex*, the *nidopallium caudolaterale* (NCL) is reciprocally connected with the equivalent of the pyramidal layer (layer V) of mammalian *premotor cortex* – the *acropallium intermedium pars centrale* (Ai), that, in turn, projects to the *optic tectum* [63]. Thus, modulation of tectal activity by the NCL, responsible for higher nervous functions, is possible. Modulation of responses in the primary auditory and visual cortices by attention is known in humans [80]. Thus, one can expect existence of similar phenomenon in pigeons.

Unfortunately, our data does not allow specify the sources of high-frequency oscillations with the sufficient accuracy. Analyzing the phase reversal in Figure S13, one can tell that oscillations with reversed phase (35-85 Hz) came mostly from the location of the lateral electrodes, where as all other frequencies came somewhere from the middle line. Such conclusion can be done if we shall assume that oscillations came from a single source. However, one should not forget that interhemispheric coherence is only about 0.05-0.15 at high frequencies. That means that a significant part of these oscillations is generated in the hemispheres independently. In such situation one differential pair of electrodes per hemisphere is not enough to detect where the signal came from. Analysis of the signals from the caudal electrodes (1, 4 in Figure S2) occurred difficult because of their high coherence with the myogram (data not shown). One can also note that the place of their implantation was not ideal: because of cavities in the pigeon skull screws were fixed in the bone and did not touch the

brain. I.e. electrodes over cerebellum were not real epidural electrodes. For sources localization it would be better to have these additional electrodes somewhere over cerebrum.

A recently done investigation of immediately early genes (IEG) expression evoked by different stimulations allowed estimate the degree of involvement of different areas in the processing of visual information [81]. Some of discovered areas are parts of known visual pathways. They include: 1) the nidopallium and ventral mesopallium, which are part of the tectofugal visual pathway; 2) the posterior part of the medial hyperpallium (also known as the visual Wulst) and the adjusted posterior dorsal mesopallium, which are the part of the thalamofugal visual pathway; and 3) cluster N, consisting of regions within the most posterior end of the hyperpallium and adjacent dorsal mesopallium, known to be activated by dim-light, night-vision in migratory songbirds and implicated in light-mediated magnetic compass detection [81-83]. Interestingly, not much expression was observed in the *optic tectum* that is definitely stimulated when something appears in the visual field. The most probable explanation of this can be driven from the fact that the expression of IEG is a marker of plastic changes in the nervous system, linked with selective strengthening of neuronal connections and memory formation. Plastic changes are always linked with the increased neuronal activity. However, not every neuronal activity is associated with the neuronal plasticity. For this reason activation of IEG may not be observed in the *optic tectum* and, thus, IEG may be difficult to use as a measure of its activity.

## Supplemental References

26. Deng, C., and Rogers, L.J. (2000). Organization of intratelencephalic projections to the visual Wulst of the chick. *Brain Res* 856, 152-162.
27. Kirsch, J.A., and Gunturkun, O. (2005). Neuronal synchronicity in the pigeon "prefrontal cortex" during learning. *Brain Res Bull* 66, 348-352.
28. Diekamp, B., Prior, H., Ioale, P., Odetti, F., Gunturkun, O., and Gagliardo, A. (2002). Effects of monocular viewing on orientation in an arena at the release site and homing performance in pigeons. *Behav Brain Res* 136, 103-111.
29. Smith, J.L., Edgerton, V.R., Betts, B., and Collatos, T.C. (1977). EMG of slow and fast ankle extensors of cat during posture, locomotion, and jumping. *J Neurophysiol* 40, 503-513.
30. Freeman, W.J., Rogers, L.J., Holmes, M.D., and Silbergeld, D.L. (2000). Spatial spectral analysis of human electrocorticograms including the alpha and gamma bands. *J Neurosci Methods* 95, 111-121.
31. Leopold, D.A., Murayama, Y., and Logothetis, N.K. (2003). Very slow activity fluctuations in monkey visual cortex: implications for functional brain imaging. *Cereb Cortex* 13, 422-433.
32. McFadden, S.A., and Reymond, L. (1985). A further look at the binocular visual field of the pigeon (*Columba livia*). *Vision Res* 25, 1741-1746.
33. Keyzers, C., Diekamp, B., and Gunturkun, B. (2000). Evidence for physiological asymmetries in the intertectal connections of the pigeon (*Columba livia*) and their potential role in brain lateralisation. *Brain Res* 852, 406-413.
34. Manns, M., Freund, N., Patzke, N., and Gunturkun, O. (2007). Organization of telencephalotectal projections in pigeons: Impact for lateralized top-down control. *Neuroscience* 144, 645-653.
35. Karten, H.J., and Hodos, W. (1967). A stereotaxic atlas of the brain of the pigeon (*Columbia livia*). (Baltimore, MD: Johns Hopkins Press).
36. Rattenborg, N.C., Obermeyer, W.H., Vacha, E., and Benca, R.M. (2005). Acute effects of light and darkness on sleep in the pigeon (*Columba livia*). *Physiol Behav* 84, 635-640.
37. Van Twyver, H., and Allison, T. (1972). A polygraphic and behavioral study of sleep in the pigeon (*Columba livia*). *Exp Neurol* 35, 138-153.
38. Hyvarinen, A., Karhunen, J., and Oja, E. (2001). Independent Component Analysis, (New York: John Wiley & Sons, Inc.).
39. Shimizu, T., Bowers, A.N., Budzynski, C.A., Kahn, M.C., and Bingman, V.P. (2004). What does a pigeon (*Columba livia*) brain look like during homing? selective examination of ZENK expression. *Behav Neurosci* 118, 845-851.
40. Siegel, J.J., Nitz, D., and Bingman, V.P. (2000). Hippocampal theta rhythm in awake, freely moving homing pigeons. *Hippocampus* 10, 627-631.
41. O'Keefe, J., and Recce, M.L. (1993). Phase relationship between hippocampal place units and the EEG theta rhythm. *Hippocampus* 3, 317-330.
42. Lachaux, J.P., George, N., Tallon-Baudry, C., Martinerie, J., Hugueville, L., Minotti, L., Kahane, P., and Renault, B. (2005). The many faces of the gamma band response to complex visual stimuli. *Neuroimage* 25, 491-501.
43. Gruber, T., Muller, M.M., Keil, A., and Elbert, T. (1999). Selective visual-spatial attention alters induced gamma band responses in the human EEG. *Clin Neurophysiol* 110, 2074-2085.

44. Sokolov, A., Pavlova, M., Lutzenberger, W., and Birbaumer, N. (2004). Reciprocal modulation of neuromagnetic induced gamma activity by attention in the human visual and auditory cortex. *Neuroimage* 22, 521-529.
45. Haenschel, C., Baldeweg, T., Croft, R.J., Whittington, M., and Gruzelier, J. (2000). Gamma and beta frequency oscillations in response to novel auditory stimuli: A comparison of human electroencephalogram (EEG) data with in vitro models. *Proc Natl Acad Sci U S A* 97, 7645-7650.
46. Chen, A.C., and Herrmann, C.S. (2001). Perception of pain coincides with the spatial expansion of electroencephalographic dynamics in human subjects. *Neurosci Lett* 297, 183-186.
47. Bauer, M., Oostenveld, R., Peeters, M., and Fries, P. (2006). Tactile spatial attention enhances gamma-band activity in somatosensory cortex and reduces low-frequency activity in parieto-occipital areas. *J Neurosci* 26, 490-501.
48. Caplan, J.B., Madsen, J.R., Raghavachari, S., and Kahana, M.J. (2001). Distinct patterns of brain oscillations underlie two basic parameters of human maze learning. *J Neurophysiol* 86, 368-380.
49. Jensen, O., Kaiser, J., and Lachaux, J.P. (2007). Human gamma-frequency oscillations associated with attention and memory. *Trends Neurosci* 30, 317-324.
50. Dell'ariccia, G., Dell'omo, G., and Lipp, H.P. (2009). The influence of experience in orientation: GPS tracking of homing pigeons released over the sea after directional training. *J Exp Biol* 212, 178-183.
51. Engelage, J., and Bischof, H.-J. (1993). The organization of the tectofugal pathway in birds: a comparative review. In *Vision, brain, and behavior in birds*, H.P. Zeigler and H.-J. Bischof, eds. (London: A Bradford Book), pp. 137-158.
52. Remy, M., and Watanabe, S. (1993). Two eyes and one world: studies of interocular and intraocular transfer in birds. In *Vision, brain, and behavior in birds*, H.P. Zeigler and H.-J. Bischof, eds. (London: A Bradford Book), pp. 333-350.
53. Bressler, S.L. (1990). The gamma wave: a cortical information carrier? *Trends Neurosci* 13, 161-162.
54. Neuenschwander, S., and Varela, F.J. (1993). Visually triggered neuronal oscillations in the pigeon: an autocorrelation study of tectal activity. *Eur J Neurosci* 5, 870-881.
55. Neuenschwander, S., Martinerie, J., Renault, B., and Varela, F.J. (1993). A dynamical analysis of oscillatory responses in the optic tectum. *Brain Res Cogn Brain Res* 1, 175-181.
56. Neuenschwander, S., Engel, A.K., Konig, P., Singer, W., and Varela, F.J. (1996). Synchronization of neuronal responses in the optic tectum of awake pigeons. *Vis Neurosci* 13, 575-584.
57. Marin, G., Mpodozis, J., Sentis, E., Ossandon, T., and Letelier, J.C. (2005). Oscillatory bursts in the optic tectum of birds represent re-entrant signals from the nucleus isthmi pars parvocellularis. *J Neurosci* 25, 7081-7089.
58. Diekamp, B., Kalt, T., and Gunturkun, O. (2002). Working memory neurons in pigeons. *J Neurosci* 22, RC210.
59. Kalt, T., Diekamp, B., and Gunturkun, O. (1999). Single unit activity during a Go/NoGo task in the "prefrontal cortex" of pigeons. *Brain Res* 839, 263-278.
60. Kalenscher, T., Diekamp, B., and Gunturkun, O. (2003). Neural architecture of choice behaviour in a concurrent interval schedule. *Eur J Neurosci* 18, 2627-2637.
61. Hartmann, B., and Gunturkun, O. (1998). Selective deficits in reversal learning after neostriatum caudolaterale lesions in pigeons: possible behavioral equivalencies to the mammalian prefrontal system. *Behav Brain Res* 96, 125-133.
62. Kalenscher, T., Ohmann, T., and Gunturkun, O. (2006). The neuroscience of impulsive and self-controlled decisions. *Int J Psychophysiol* 62, 203-211.

63. Kroner, S., and Gunturkun, O. (1999). Afferent and efferent connections of the caudolateral neostriatum in the pigeon (*Columba livia*): a retro- and anterograde pathway tracing study. *J Comp Neurol* 407, 228-260.
64. Siegel, J.J., Nitz, D., and Bingman, V.P. (2002). Electrophysiological profile of avian hippocampal unit activity: a basis for regional subdivisions. *J Comp Neurol* 445, 256-268.
65. Cheng, K., Spetch, M.L., Kelly, D.M., and Bingman, V.P. (2006). Small-scale spatial cognition in pigeons. *Behav Processes* 72, 115-127.
66. Hough, G.E., and Bingman, V.P. (2008). Rotation of visual landmark cues influences the spatial response profile of hippocampal neurons in freely-moving homing pigeons. *Behav Brain Res* 187, 473-477.
67. Kahn, M.C., Siegel, J.J., Jechura, T.J., and Bingman, V.P. (2008). Response properties of avian hippocampal formation cells in an environment with unstable goal locations. *Behav Brain Res* 191, 153-163.
68. Nardi, D., and Bingman, V.P. (2007). Asymmetrical participation of the left and right hippocampus for representing environmental geometry in homing pigeons. *Behav Brain Res* 178, 160-171.
69. Siegel, J.J., Nitz, D., and Bingman, V.P. (2006). Lateralized functional components of spatial cognition in the avian hippocampal formation: evidence from single-unit recordings in freely moving homing pigeons. *Hippocampus* 16, 125-140.
70. Prechtl, J.C., Cohen, L.B., Pesaran, B., Mitra, P.P., and Kleinfeld, D. (1997). Visual stimuli induce waves of electrical activity in turtle cortex. *Proc Natl Acad Sci U S A* 94, 7621-7626.
71. Sieck, M.H., and Wenzel, B.M. (1969). Electrical activity of the olfactory bulb of the pigeon. *Electroencephalogr Clin Neurophysiol* 26, 62-69.
72. Pollok, B., Gross, J., Muller, K., Aschersleben, G., and Schnitzler, A. (2005). The cerebral oscillatory network associated with auditorily paced finger movements. *Neuroimage* 24, 646-655.
73. Courtemanche, R., and Lamarre, Y. (2005). Local field potential oscillations in primate cerebellar cortex: synchronization with cerebral cortex during active and passive expectancy. *J Neurophysiol* 93, 2039-2052.
74. Witham, C.L., and Baker, S.N. (2007). Network oscillations and intrinsic spiking rhythmicity do not covary in monkey sensorimotor areas. *J Physiol* 580, 801-814.
75. Middleton, S.J., Racca, C., Cunningham, M.O., Traub, R.D., Monyer, H., Knopfel, T., Schofield, I.S., Jenkins, A., and Whittington, M.A. (2008). High-frequency network oscillations in cerebellar cortex. *Neuron* 58, 763-774.
76. De Zeeuw, C.I., Hoebeek, F.E., and Schonewille, M. (2008). Causes and consequences of oscillations in the cerebellar cortex. *Neuron* 58, 655-658.
77. de Solages, C., Szapiro, G., Brunel, N., Hakim, V., Isope, P., Buisseret, P., Rousseau, C., Barbour, B., and Lena, C. (2008). High-frequency organization and synchrony of activity in the purkinje cell layer of the cerebellum. *Neuron* 58, 775-788.
78. Paulson, G. (1964). The Avian Eeg: An Artifact Associated with Ocular Movement. *Electroencephalogr Clin Neurophysiol* 16, 611-613.
79. Letelier, J.C., Marin, G., Sentis, E., Tenreiro, A., Fredes, F., and Mpodozis, J. (2004). The mapping of the visual field onto the dorso-lateral tectum of the pigeon (*Columba livia*) and its relations with retinal specializations. *J Neurosci Methods* 132, 161-168.
80. Poghosyan, V., and Ioannides, A.A. (2008). Attention modulates earliest responses in the primary auditory and visual cortices. *Neuron* 58, 802-813.
81. Feenders, G., Liedvogel, M., Rivas, M., Zapka, M., Horita, H., Hara, E., Wada, K., Mouritsen, H., and Jarvis, E.D. (2008). Molecular mapping of movement-associated areas in the avian brain: a motor theory for vocal learning origin. *PLoS ONE* 3, e1768.

82. Mouritsen, H., Feenders, G., Liedvogel, M., Wada, K., and Jarvis, E.D. (2005). Night-vision brain area in migratory songbirds. *Proc Natl Acad Sci U S A* 102, 8339-8344.
83. Heyers, D., Manns, M., Luksch, H., Gunturkun, O., and Mouritsen, H. (2007). A visual pathway links brain structures active during magnetic compass orientation in migratory birds. *PLoS ONE* 2, e937.